Assessing Climate Change Impacts on Live Fuel Moisture and Wildfire Risk Using a Hydrodynamic Vegetation Model

Wu Ma[1], Lu Zhai[2], Alexandria Pivovaroff[3], Jacquelyn Shuman[4], Polly Buotte[5], Junyan Ding[6], Bradley Christoffersen[7], Ryan Knox[6], Max Moritz[8], Rosie A. Fisher[9], Charles D. Koven[6], Lara Kueppers[10], Chonggang Xu[1,*]

[1] *Earth and Environmental Sciences Division, Los Alamos National Laboratory, Los Alamos, NM, United States*

[2] *Department of Natural Resource Ecology and Management, Oklahoma State University, Stillwater, OK, United States*

[3] *Atmospheric Science and Global Change Division, Pacific Northwest National Laboratory, Richland, WA, United States*

[4] *National Center for Atmospheric Research, Climate and Global Dynamics, Terrestrial Sciences Section, Boulder, CO, United States*

[5] *Energy and Resources Group, University of California, Berkeley, CA, United States*

[6] *Climate and Ecosystem Sciences Division, Lawrence Berkeley National Laboratory, CA, United States*

[7] *Department of Biology, University of Texas Rio Grande Valley, Edinburg, TX, United States*

[8] *UC ANR Cooperative Extension, Bren School of Environmental Science & Management, University of California, Santa Barbara, CA, United States*

[9] *Centre Européen de Recherche et de Formation Avancée en Calcul Scientifique, Toulouse, France*

[10]~~[9]~~ *Energy and Resources Group, University of California, Berkeley, and Lawrence Berkeley National Laboratory, Berkeley, CA, United States*

* Corresponding author (Chonggang Xu, cxu@lanl.gov)

Abstract: Live fuel moisture content (LFMC) plays a critical role in wildfire dynamics, but little is known about responses of LFMC to multivariate climate change, e.g., warming temperature, CO_2 fertilization and altered precipitation patterns, leading to a limited prediction ability of future wildfire risks. Here, we use a hydrodynamic demographic vegetation model to estimate LFMC dynamics of chaparral shrubs, a dominant vegetation type in fire-prone southern California. We parameterize the model based on observed shrub allometry and hydraulic traits, and evaluate the model's accuracy through comparisons between observed ~~simulated~~ and simulated ~~observed~~ LFMC of three plant functional types (PFTs) under current climate conditions. Moreover, we estimate the number of days per year of LFMC below 79% (which is a critical threshold for wildfire danger rating of southern California chaparral shrubs) from ~~1950~~ 1960 to 2099 for each PFT, and compare the number of days below the threshold for medium and high greenhouse gas emission scenarios (RCP4.5 and 8.5). We find that climate change could lead to more days per year (5.~~5~~2-~~15~~14.~~2~~8% increase) with LFMC below 79% between the ~~from~~ historical ~~period (1950~~1960-1999) and~~to~~ future ~~period (2075~~2080-2099) periods, implying~~and therefore cause~~ an increase in wildlife danger for chaparral shrubs in southern California. Under the high greenhouse gas emission scenario during the dry season, we find that the future LFMC reductions mainly result from a warming temperature, which leads to 9.~~5~~1-~~19~~18.~~1~~6% reduction in LFMC. Lower precipitation in the spring leads to a 6.~~6~~3-8.~~3~~1% reduction in LFMC. The combined impacts of warming and precipitation change on fire season length are equal to the additive impacts of warming and precipitation change individually. Our results show that the CO_2 fertilization will mitigate fire risk by causing a 3.~~7~~5-~~5~~4.~~1~~8% increase in LFMC. Our

results suggest that multivariate climate change could cause a significant net reduction in LFMC and thus exacerbate future wildfire danger in chaparral shrub systems.

Keywords: FATES-HYDRO, chaparral shrubs, plant functional types, southern California, CO$_2$ enrichment, climate change

1. Introduction

Historical warming and changes in precipitation have already impacted wildfire at a global scale (e.g. Stocks et al. 1998; Gillett et al. 2004; Westerling et al. 2003, 2006) and it is expected that accelerating future warming will continue to significantly influence global wildfire regimes (e.g. Flannigan et al. 2009; Liu et al. 2010; Moritz et al. 2012). So far, prior studies have mainly focused on impacts of dead fuel moisture, fuel loads, and weather conditions on wildfire. Limited studies have applied proxies of live fuel moisture in global-fire models. For example, dead fuel moisture is found to be related to fire ignition and fire spread potential (or potential area burnt) (Aguado et al. 2007~~; Caccamo et al. 2012a~~), ~~and~~ specific weather conditions such as increased vapor pressure deficit (Williams et al. 2019) can lead to a vast increase in fire activity (Goss et al. 2020), and wildfire fuel loads are projected to increase under climate change (Matthews et al. 2012; Clarke et al. 2016). In global-fire models, studies have used proxies of live fuel moisture (Bistinas et al. 2014; Kelley et al. 2019) as well as explicit representation of live fuels (Hantson et al. 2016; Rabin et al. 2017). While previous studies provide great insights into fire risks with changes in climate, ~~and~~ dead fuel moisture, fuel loads, and representation of live fuel moisture, there is still limited understanding of how climate change influences live fuel moisture content (LFMC) and the consequent wildfire risks. This is particularly true for the combined impacts of warming temperature, altered precipitation, and increasing CO$_2$ fertilization

(Chuvieco et al. 2004; Pellizzaro 2007; Caccamo et al. 2012a, ~~Caccamo et al. 2012~~b; Williams et al. 2019; Goss et al. 2020).

A measure of water content within living ~~leaves and fine branches~~plant tissue in relation to their dry weight, LFMC has been found to be one of the most critical factors influencing combustion, fire spread, and fire consumption (e.g. Agee et al. 2002; Zarco-Tejada et al. 2003; Bilgili & Saglam 2003; Yebra et al. 2008; Dennison et al. 2008; Anderson & Anderson 2010; Keeley et al. 2011). This is because a low LFMC~~fuel moisture content~~ leads to increased flammability and a higher likelihood of ignition (Dimitrakopoulos & Papaioannou 2001). For instance, LFMC was found to be a significant factor contributing to the occurrence of wildfires in Australia (Plucinski 2003; Nolan et al. 2016; Yebra et al. 2018; Rossa & Fernandes 2018; Pimont et al. 2019), Spain (Chuvieco et al. 2009) and California (Santa Monica Mountains; Dennison et al. 2008; Dennison & Moritz 2009; Pivovaroff et al. 2019). Dennison & Moritz (2009) found strong evidence of a LFMC threshold~~, but near~~ (79%) for southern California chaparral shrubs, which may determine when large fires can occur in this region.

Vegetation moisture content is dependent on both ecophysiological characteristics of the species and environmental conditions, including both climatic variables and soil water availability (Rothermel 1972; Castro et al. 2003; Castro et al. 2003; Pellizzaro 2007; Pivovaroff et al. 2019; Nolan et al. 2020). So far, little is known about the relative importance of different climate variables to future LFMC dynamics. On the one hand, warming could contribute to a higher atmospheric demand and higher evapotranspiration (Rind et al. 1990) and thus lead to a lower LFMC. On the other hand, higher CO_2 concentration will decrease stomatal conductance (Wullschleger et al. 2002) and plant water loss, and thus lead to a higher LFMC. The impacts of

CO_2 and warming could be complicated by local changes in precipitation patterns and humidity (Mikkelsen et al. 2008).

The sensitivity of LFMC to climate change is likely to be affected by plant hydraulic traits (~~PFT,~~ the plant properties that regulate water transport and storage within plant tissues), which affect plant water regulation (Wu et al. 2020). Variations in ~~Hydraulic~~ hydraulic traits ~~determine~~ reflect contrasting plant drought adaptation strategies when responding to dry conditions. Two contrasting overall strategies are: 1) water stress avoiders and 2) water stress tolerators (Tobin et al. 1999; Wei et al. 2019). The “avoiders” are generally characterized by ~~have~~ a more conservative hydraulic strategy under water stress by either closing stomata early, dropping leaves or accessing deep water to avoid more negative water potentials and therefore xylem cavitation. Meanwhile, the “tolerators” typically ~~generally have a more aggressive hydraulic strategy by~~ build~~ing~~ xylem and leaves that are more resistant to cavitation so that they can tolerate more negative water potential and continue to conduct photosynthesis under water stress. Therefore, compared with the tolerators, the avoiders normally have a lower sapwood density and higher plant water storage capacity in their tissues to avoid cavitation (Meinzer et al. 2003, 2009; Pineda-Garcia et al. 2013). Because the avoiders rely on water storage capacity as one way to avoid cavitation thereby maintaining a relatively high LFMC, and water loss from storage should increase with warming, LFMC could~~should~~ be more sensitive to climate change in avoiders relative to tolerators.

While over half of terrestrial landscapes on Earth are considered fire-prone (Krawchuk et al. 2009), Mediterranean-type climate regions are routinely impacted by fire, often on an annual basis. This is partly because Mediterranean climate regions are characterized by winter rains followed by annual dry season~~summer~~ ~~drought~~, when little to no rainfall occurs for several months. Multiday periods of extreme high temperatures, as well as katabatic hot, dry, and intense winds, often punctuate the annual drought, leading to some of the worst fire weather in the world (Schroeder et al. 1964). This can result in wildfires that are large, high-intensity, and stand-replacing (Keeley 1995; Keeley & Zedler 2009; Balch et al. 2017). Globally, Mediterranean climate regions are characterized by evergreen sclerophyllous-leaved shrublands. The Mediterranean climate region in California is dominated by chaparral, which is adapted to the periodic fire regime in California (Venturas et al. 2016). Previous studies have proposed a variety of relationships between chaparral LFMC and fire danger in southern California (Dennison et al. 2008; Dennison & Moritz 2009), but less is known about how climate changes could alter LFMC and fire danger. In chaparral, LFMC is usually high during the winter and spring (wet season) and then gradually declines during the dry season (summer and fall), which leads to a typical fire season approximately six months long in southern California (Pivovaroff et al. 2019). One key risk is that severe drought conditions are becoming exacerbated under climate change, which might lead to the occurrence of larger and higher-intensity fires in chaparral (Dennison et al. 2008; Dennison & Moritz 2009).

There has been a long history of wildfire modeling, with three types of models: 1) fine-scale fire behavior models (e.g. FIRETEC by Linn et al. 2002); 2) landscape-scale fire disturbance models (e.g. LANDIS-II by Sturtevant et al. 2009); and 3) global-scale fire dynamics models (e.g. Hantson et al. 2016; Rabin et al. 2017; SPITFIRE by Thonicke et al. 2010). While these models focus on simulation at different scales, fire measures of the simulation ~~their fire danger indices~~ are mainly calculated from climate and dead fuel moisture and currently lack ~~dynamic~~ prediction of LFMC dynamics. One key limitation is that most previous models have not yet considered plant hydrodynamics (Holm et al. 2012; Xu et al. 2013; Seiler et al. 2014), which is integral to LFMC prediction. Recently, there have been important improvements to global dynamic and demographic vegetation models by incorporating plant hydrodynamics (McDowell et al. 2013; Xu et al. 2016; Fisher et al. 2018; Mencuccini et al. 2019). These models have been used to study the interaction between elevated CO_2 and drought (Duursma & Medlyn, 2012), the impact of hydraulic traits on plant drought response (Christofferson et al. 2016), the role of hydraulic diversity in vegetation response to drought (Xu et al. 2016) and hydroclimate change (Powell et al. 2018), and vegetation water stress and root water uptake (Kennedy et al. 2019). While the main purpose of the new hydraulic components is to improve the vegetation response to drought, the fact that hydrodynamic models consider tissue water content as a prognostic variable provides an opportunity to assess the climate impacts on LFMC.

The objective of this study is to quantify LFMC dynamics and associated changes in fire season duration for a chaparral ecosystem in southern California under climate change using a vegetation demographic model (that resolves the size and age-since-disturbance structure of plant populations) (Xu et al. 2016; Fisher et al. 2018) that incorporates plant hydraulics. We test one overarching hypothesis: future climate change will decrease LFMC and consequently result in a longer fire season as determined by a critical threshold of LFMC (H_0). Specifically, we test the following four sub-hypotheses: 1) warming has a stronger impact on LFMC than CO_2 fertilization (H_1); 2) the reductions in spring and autumn precipitation~~seasonal changes in precipitation~~ lead to a longer fire season as determined by LFMC (H_2); 3) the combined impacts of warming and precipitation on fire season length are equal to the additive impacts of warming and precipitation change individually (H_3); and 4) plants with more conservative hydraulic strategies (“avoiders”) will be more vulnerable~~sensitive~~ to warming ~~because their higher water storage capacity could be more vulnerable to warming~~ (H_4).

2. Materials and Methods

To understand climate change impacts on LFMC for the chaparral ecosystem, we applied the Functionally Assembled Terrestrial Simulator (FATES; Fisher et al. 2015; Massoud et al. 2019; Koven et al. 2020) coupled with a hydrodynamic vegetation module (FATES-HYDRO; Christoffersen et al. 2016) in the Santa Monica Mountains in California. We validated the model using the observed LFMC for three chaparral shrub plant functional types (PFTs). Then, we applied FATES-HYDRO to estimate long-term dynamics of leaf water content (L~~FM~~WC) during ~~1950~~1960-2099 for each PFT using downscaled Earth System Model (ESM) climate scenarios. We converted simulated leaf water content (LWC) to LFMC within leaves and shoots. Based on the simulated LFMC, we evaluated wildfire danger based on the number of days per year of LFMC below the critical value of 79% from ~~1950~~ 1960 to 2099 for each PFT under RCP 4.5 and 8.5. Finally, we assessed the relative importance of changes in individual and combined climate variables including CO_2, temperature, precipitation, and relative humidity and tested the corresponding hypotheses.

2.1 Study site

The study site is located at the Stunt Ranch Santa Monica Mountains Reserve, in the Santa Monica Mountains in California, USA (N 34° 05’, W 118° 39’). Stunt Ranch is dominated by chaparral vegetation, with an elevation of approximately 350 m, a west-facing slope, and a Mediterranean-type climate. The study site harbors an abundance of fauna, particularly birds and reptiles. ~~The average maximum temperature is 31.5 °C and the average minimum temperature is 4.6 °C.~~ The mean annual temperature is 18.1°C. The ~~Mean~~ mean annual precipitation is 478 mm, occurring mostly during the wet season (i.e. November-March) with almost no rainfall during the dry season (i.e. April-October). Stunt Ranch last burned in year 1993 but has recovered well.

~~Soil texture information for Stunt Ranch is based on a national soil survey database (https://websoilsurvey.sc.egov.usda.gov/App/WebSoilSurvey.aspx; Table S1).~~ We focused on PFTs representing 11 study species (Fig. 1), including chamise (*Adenostoma fasciculatum* - Af), red shank (*Adenostoma sparsifolium* - As), big berry manzanita (*Arctostaphylos glauca* - Ag), buck brush (*Ceanothus cuneatus* - Cc), greenbark ceanothus (*Ceanothus spinosus* - Cs), mountain mahogany (*Cercocarpus betuloides* - Cb), toyon (*Heteromeles arbutifolia* - Ha), laurel sumac (*Malosma laurina* - Ml), scrub oak (*Quercus berberidifolia* - Qb), hollyleaf redberry (*Rhamnus ilicifolia* - Ri), and sugar bush (*Rhus ovata* - Ro). Detailed information about the study site and species characterizations found at Stunt Ranch can be found in Venturas et al. (2016) and Pivovaroff et al. (2019).

2.2 FATES-HYDRO model

FATES is a vegetation demographic model (Fisher et al. 2015), which uses a size-structured group of plants (cohorts) and successional trajectory-based patches based on~~using~~ the ecosystem demography approach (Moorcroft et al. 2001~~; Massoud et al. 2019~~). FATES simulates the demographic process including seed production, seed emergence, growth and mortality ~~in part by integrating photosynthesis across different leaf layers for each cohort. FATES allocates photosynthetic carbon to storage and leaf, root, and stem tissues based on the allometry of different plant species~~ (Koven et al. 2020). Because the main purpose is to assess LFMC, we controlled for variation in plant size structure that could arise from plant traits or climate differences between model runs by using a reduced-complexity configuration of the model where growth and mortality are turned off and ecosystem structure is held constant. ~~Mortality within FATES is mainly simulated by carbon starvation caused by depletion of carbon storage and hydraulic function failure caused by embolism via the hydrodynamic model (Christoffersen et al.~~

~~2016).~~ FATES has to be hosted by a land surface model to simulate the soil hydrology, canopy temperature and transpiration. These host land models include~~is coupled~~ ~~with~~ the Exascale Energy Earth System Model (E3SM, Caldwell et al., 2019) land model (ELM) as well as the Community Earth System Model (Fisher et al 2015) and the Norwegian Earth system model (NorESM, Tjiputra et al 2013). In this study, we used the DOE-sponsored ELM as our host land model. The time step of FATES to calculate carbon and water fluxes is 30 minutes and it can downscale the data from 6-hourly climate drivers.

A key component of FATES, the plant hydrodynamic model (~~HYDRO~~HYDRO, based on~~;~~ Christoffersen et al. 2016), simulates the water flow from soil through root, stem and leaf to the atmosphere. In this model, water flow is calculated based on water pressure gradients across different plant compartments (leaf, stem, transporting roots, absorbing roots and rhizosphere). Specifically, flow between compartment i and $i + 1$ (Q_i) is given by

$$Q_i = -K_i \Delta h_i \tag{1}$$

where K_i is the total conductance (kg MPa^{-1} s^{-1}) at the boundary of compartments i and $i+1$ and Δh_i is the total water potential difference between the compartments:

$$\Delta h_i = \rho_w g(z_i - z_{i+1}) + (\psi_i - \psi_{i+1}) \tag{2}$$

where z_i is compartment distance above (+) or below (-) the soil surface (m), ρ_w is the density of water (10^3 kg m^{-3}), g is acceleration due to gravity (9.8 m s^{-2}), and ψ_i is tissue or soil matric water potential (MPa). K_i is treated here as the product of a maximum boundary conductance between compartments i and $i+1$ ($K_{max,i}$), and the fractional maximum hydraulic conductance of the adjacent compartments (FMC_i or FMC_{i+1}), which is a function of the tissue water content. A key parameter that controls FMC is the critical water potential (P_{50}) that leads to 50% loss of hydraulic conductivity. The tissue water potential is calculated based on pressure-volume (PV) theory (Tyree & Hammel, 1972; Tyree & Yang, 1990; Bartlett et al., 2012). For leaves, it is described by three phases: 1) capillary water phase with full turgor, 2) elastic drainage phase before reaching turgor loss point; and 3) post-turgor loss phase. For other tissues, it only has phases 2 and 3. Compared to a non-hydrodynamic model, this formulation allows the simulation of plant water transport limitation on transpiration. For the non-hydrodynamic version of FATES, the water limitation factor for transpiration (B_{tran}) is calculated based on the soil moisture potential (Fisher et al. 2015). For the hydrodynamic version, B_{tran} is calculated based on the leaf water potential (ψ_l) (Christoffersen et al. 2016) as follows,

$$B_{tran} = [1 + (\frac{\psi_l}{P_{50\_gs}})^{a_l}]^{-1} \cancel{,} \qquad (3)$$

where P_{50_gs} is the leaf water potential that leads to 50% loss of stomatal conductance and a_l is the shape parameter. Please refer to Christoffersen, et al. 2016 for details of formulations of FMC for different plant tissues.

~~Because the main purpose here is to assess LFMC, we controlled for variation in size structure that could arise from hydrodynamic trait or climate differences between model runs by using a reduced-complexity configuration of the model where growth and mortality are turned off and ecosystem structure is held constant. The plant sizes and number density are set based on a vegetation inventory from Venturas et al. (2016).~~

2.3 Allometry and trait data for model parameterization

FATES-HYDRO has a large number of parameters (>80; see Massoud et al. 2019 for a complete list except for hydraulic parameters). Based on a previous sensitivity analysis study (Massoud et al. 2019), we focused our parameter estimation efforts on ~~estimating~~ the most influential parameters for allometry, leaf and wood traits, and hydraulic traits from observations of 11 chaparral shrub species (see Supplementary, Table S2), collected from Jacobsen et al. (2008) and Venturas et al. (2016). For this study, w~~W~~e assumed that the allometry of a shrub is analogous to that of a small tree. However, we did make several important modifications to accommodate the allometry of shrub as their height and crown area relationships to diameter could be different from trees. First, instead of using the diameter at breast height as the basis for allometry to calculate the height, crown area and leaf biomass, we used the basal diameter as the basis for shrubs. Second, in the allometry of trees, the diameter for maximum height ($d_{1:}$ Fates_allom_dbh_maxheight, Table S1) is the same as the diameter for maximum crown area ($d_{2:}$ Fates_allom_d2ca_max, Table S1). As our data showed that d_1 and d_2 are different for shrubs, we have modified the codes so that the d_1 and d_2 can be set for different values. It is possible that different branching and path length patterns for stems of chaparral species could impact the hydraulics compared to trees; however, FATES-HYDRO treats all the aboveground xylem as a single pool and thus it should not affect our model simulation results.

Based on a hierarchical cluster analysis (Bridges 1966) of allometry and trait data, there are a clear separation among the shrub species. First, the dendrogram is built and every data point finally merges into a single cluster with the height shown on the y-axis. Then we cut the dendrogram in order to create the desired number of clusters determined by a pragmatic choice based on hydraulic traits of eleven chaparral shrub species (Fig. 1). R's rect.hclust~~()~~ function (https://www.rdocumentation.org/packages/stats/versions/3.6.2/topics/rect.hclust) was used to see the clusters on the dendrogram. All parameters of allometry, leaf and wood traits, and hydraulic traits were collected from observations shown in the Table S2 and S3 of the supplementary. According to the principle of model parsimony, we do not want to classify the species into more than 3 PFTs. Meanwhile, we also want to differentiate the fundamental plant growth and water use strategies that will determine plant transpiration rate and the corresponding LFMC. If we choose to classify the species into two PFTs (based on the solid horizontal line in Fig. 1), then we will not be able to differential species with aggressive and conservative hydraulic strategy in the second group and not be able to test H4. Therefore, the chaparral shrub species were classified into three PFTs (based on the dotted horizontal line in Fig. 1 and Table S3), that are able to differential plant growth and hydraulic strategy. The three PFTs include~~:~~ a low productivity, aggressive drought tolerance hydraulic strategy PFT (PFT-~~–~~L~~P~~A~~H~~) with a relative low $V_{c,max25}$ (the maximum carboxylation rate at 25 ^{o}C) and a very negative P_{50} (the leaf water potential leading to 50% loss of hydraulic conductivity); a medium productivity, conservative drought tolerance hydraulic strategy PFT (PFT-~~–~~M~~P~~C~~H~~) represented by a medium $V_{c,max25}$ and a less negative P_{50}, turgor loss point and water potential at full turgor; and a high productivity, aggressive drought tolerance hydraulic strategy PFT (PFT-~~–~~H~~P~~A~~H~~) with a relatively high $V_{c,max25}$ and a very negative P_{50}. The mean of species-level trait data weighted by species abundance at the site were used to parameterize FATES-HYDRO.

2.4 Model initialization

Our model simulation is transient in terms of soil water content, leaf water content, carbon and water fluxes. The forest structure (plant sizes and number density) is fixed and is parameterized based on a vegetation inventory from Venturas et al. (2016). The soil texture and depth information are parameterization based on a national soil survey database (https://websoilsurvey.sc.egov.usda.gov/App/WebSoilSurvey.aspx; Table S1). The soil moisture is initialized with 50% of the saturation and the tissue plant water content is initialized so that it is in equilibrium with the soil water potential. We run the model for 10 years based on 1950-

1960 climate so that the simulated soil moisture, leaf water content, carbon and water fluxes are not depending on their initial conditions.

2.~~4~~ 5 Live Fuel Moisture Content for model ~~evaluation~~validation

In this study, we used measured LFMC to validate simulated LFMC~~,~~. ~~In the~~ FATES-HYDRO~~, the model~~ does~~id~~ not directly simulate the LFMC. Thus, we estimated the LFMC based on simulated LWC~~predictions~~. The LWC in the model is calculated as follows,

$$\text{LWC} = \frac{fw-dw}{dw} * 100, \qquad (4)$$

~~W~~where, *fw* is the fresh weight and *dw* is the dry weight, which are simulated within FATES-HYDRO. Then, we estimated the LFMC within leaves and shoots using the empirical equation derived from shrub LFMC and LWC data including the three regenerative strategies [seeder (S), resprouter (R) and seeder–resprouter (SR)], in summer, autumn and winter from Fig. 4 and 5 -in Saura-Mas and Lloret's study (2007) as follows (Fig. S4),

$$\text{LFMC} = 31.091 + 0.491\text{LWC}, \qquad (5)$$

The climate in -Saura-Mas and Lloret's study is Mediterranean (north-east Iberian Peninsula), which is consistent with the climate of our study area~~our study~~. ~~. LFMC (%) is the ratio of water weight to dry weight of living plant tissue (Burgan 1979).~~ LFMC was measured on our site approximately every three weeks, concurrently with plant water potentials in 2015 and 2016. LFMC measurement details can be found in ~~(~~Pivovaroff et al. (2019). For comparison with our model outputs, we calculated the mean LFMC within leaves and shoots for each PFT weighted by the species abundance (Venturas et al. 2016). Species abundance was calculated by dividing mean density of a specific species by the mean density of all species.

2.~~5~~ 6 Climate drivers

We forced the FATES-HYDRO model with 6-hourly temperature, relative humidity, precipitation, downward solar radiation, and wind components~~, and specific humidity~~. Historical climate data during 2012-2019, which were used for FATES-HYDRO calibration, were extracted from a local weather station (https://stuntranch.ucnrs.org/weather-date/). Historical and future climate data during 1950-2099, which were used for simulations of LFMC by FATES-HYDRO model, were downloaded from the Multivariate Adaptive Constructed Analogs (MACA) datasets (Abatzoglou & Brown ~~2011~~2012; http://maca.northwestknowledge.net). The MACA datasets (1/24-degree or approximately 4-km; Abatzoglou & Brown ~~2011~~2012) include 20 ESMs with historical forcings during 1950-2005 and future Representative Concentration Pathways (RCPs) RCP 4.5 and RCP8.5 scenarios during 2006-2099 from the native resolution of the ESMs. ~~As training data for MACAv1/v2-METDATA,~~ T~~t~~he gridded surface meteorological dataset METDATA (Abatzoglou, 2013) were used with high spatial resolution (1/24-degree) and daily timescales for near-surface minimum/maximum temperature, minimum/maximum relative humidity, precipitation, downward solar radiation, and wind components~~, and specific humidity~~. Then we downscaled the MACA daily data to 6-hourly based on the temporal anomaly of the observed mean daily data to the hourly data for each day during 2012-2019. The model is driven by yearly CO_2 data obtained from Meinshausen et al (2011).

2.~~6~~ 7 Hypothesis testing

To test H_0 (future climate change will decrease LFMC and consequently result in a longer fire season as determined by a critical threshold of LFMC), we compared the simulated mean LFMC, derived from modeled leaf water content, under the climate projections from 20 ESMs under RCP 4.5 and 8.5. We then tested if the LFMC during the April-October dry season in the historic period of ~~1950~~1960-1999 is significantly higher than that in the future period of ~~2075~~2080-2099. For the fire season duration, we estimated the number of days per year below a critical threshold of LFMC (79%). Similarly, we tested if the number of days per year below the critical threshold of LFMC during the historical period are significantly different from that during the future period. We used a bootstrapped approach (Jackson 1993) to test if the mean of LFMC or fire season duration are significantly different between these two periods. Specifically, we randomly draw 10000 samples from the simulated residuals of LFMCs or fire season durations estimated by 20 ESMs for these two periods under the null hypothesis that there is no difference in the mean. We then calculated p-values by comparing the simulated mean difference to the empirical distribution of difference estimated from these 10000 samples. See Supplementary section 5.2 within Xu et al. (2019) for the details.

To test H_1 (warming has a stronger impact on LFMC than CO_2 fertilization), we compared ~~model outputs of~~ mean simulated LFMC and fire season length for three PFTs with/without CO_2 changes (fixed CO_2 at 367 ppm vs dynamic CO_2 concentrations from RCP 4.5 or RCP 8.5) and warming. To remove the future warming trend, future temperature was replaced with historical (1986-2005) temperature data for every 20 year period. Similarly, to test H_2 (the reductions in spring and autumn precipitation lead to a longer fire season as determined by LFMC), we compared the model outputs of LFMC and fire season length for three PFTs with/without precipitation changes. To test H_3 (the combined impacts of warming and precipitation on fire season length are equal to the additive impacts of warming and precipitation change individually), we compared model outputs of LFMC and fire season length for three PFTs under three scenarios: 1) without warming; 2) without precipitation changes; and 3) without warming and precipitation changes. Finally, to test H_4 (plants with more conservative hydraulic strategies will be more vulnerable to warming), we compared model outputs of LFMC and fire season length across the three different PFTs with different hydraulic strategies.

3. Results

3.1 Comparison between simulated and measured LFMC

Our results showed that FATES-HYDRO was able to capture variation in the LFMC for different PFTs and soil water content in 5-cm depth (Fig. 2 and S3), also for Chamise in 2018 (Fig. S5) although we had limited observed LFMC data. Specifically, the model was able to capture ~~93~~96%, ~~88~~86%, and ~~82~~80% of the variance in observed LFMC for the period of 2015-2016 for three PFTs, respectively (Fig. 2 b, d, f). The model was also able to capture the seasonal dynamics of soil water content, LFMC, and LFMC below the threshold 79% in comparison to observed data (Fig. 2 a, c, e and S3).

3.2 Changes in the LFMC and fire season length from historical to future periods

Using the validated model driven by climate projections from 20 ESMs under greenhouse gas emission scenarios RCP4.5 and RCP 8.5, we found that the daily mean LFMC during the future period of ~~2075~~2080-2099 was projected to become significantly lower than that during the historical period of ~~1950~~1960-1999 for all three PFTs (Fig 3, P<0.000001). Our results also showed that the spread among models increase with time, suggesting a larger uncertainty in the projection into the future. Specifically, the histogram of daily mean LFMC during the April-October dry season showed that there was a higher probability of low LFMC under future climate conditions (Fig. S1). The daily mean LFMC decreased from 84.~~9~~7%, 101.~~5~~3%, and 78.~~6~~4% during the historical period of ~~1950~~1960-1999 to 81.~~3~~0-~~83~~82.~~1~~8%, 96.~~6~~3-~~99~~98.~~2~~8%, and

~~75~~74.~~1~~8-76.~~9~~6% during the future period of ~~2075~~2080-2099 under both climate scenarios for PFT-~~_~~L~~P~~A~~H~~, PFT-~~_~~M~~P~~C~~H~~, PFT-~~_~~H~~P~~A~~H~~, respectively (Fig 3).

Based on the projected LFMC, there was a significant increase in the fire season length with the critical threshold of LFMC from the historical period of ~~1950~~1960-1999 to the future period of ~~2075~~2080-2099 for three PFTs. With the critical threshold of 79% LFMC, the fire season length was projected to increase by ~~21~~20, ~~23~~22, ~~20~~ 19 days under RCP 8.5 (Fig. 4 and Table S4), and to increase by ~~10~~9, ~~12~~11, ~~9~~ 8 days under RCP 4.5 (Fig. 4 and Table S4). Our results also showed that the spread among models increase with time, suggesting a larger uncertainty in the projection into the future. The above results for mean LFMC and fire season length support hypothesis H_0 that future climate change will decrease LFMC and consequently result in a longer fire season, as determined by critical thresholds for LFMC, for all three PFTs.

3.3 Relative effects of individual climate changes on the length of the fire season

In order to better understand the relative contribution to fire season length of different climate variables, we ran FATES-HYDRO for three PFTs using meteorological forcings that isolated and removed changes in individual specific variables. Our results showed that the increase in fire season length mainly resulted from warming, which led to ~~17~~16-~~24~~ 23 days (9.~~5~~1-~~19~~18.~~1~~6%) per year increase in fire season length for the critical threshold of 79% LFMC under RCP 8.5 (Fig. 5). This is because warming is pushing Vapor Pressure Deficit (VPD)~~ ever~~ higher, resulting in increased fire season length. For RCP 4.5, the warming contributed to ~~6~~5-~~7~~ 6 days (~~4~~3.~~1~~8-4.~~7~~3%) per year increase in fire season length (Fig. 5). We also found that elevated CO_2 concentrations decreased fire season length with ~~7~~6-~~8~~ 7 days (3.~~7~~5-~~5~~4.~~1~~8%) per year decrease in fire season length under RCP 8.5 (Fig. 5). Under RCP 4.5, CO_2 increases led to 2-3 days (1.~~7~~5-2.~~4~~2%) per year decrease in fire season length (Fig. 5). Because the impact of warming on fire season length was stronger than the mitigation from CO_2 enrichment, our results support hypothesis H_1 (warming has a stronger impact on LFMC than CO_2 fertilization).

Even though total precipitation was projected to increase in the future, lower precipitation in the spring and autumn (Fig. S2 a, b) led to ~~9~~8-~~11~~ 10 days (6.~~6~~3-8.~~3~~1%) per year increase in fire season length with the critical threshold of 79% LFMC under RCP 8.5 (Fig. 5). Under RCP 4.5, the precipitation changes contributed to 1-3 days (0.~~9~~8-1.~~7~~6%) increase in fire season length (Fig. 5). This result supported hypothesis H_2 that the reductions in spring and autumn precipitation~~seasonal changes in precipitation~~ lead to a longer fire season as determined by LFMC.

Our results showed that the combined impacts of warming and precipitation on fire season length were equal to the additive impacts of warming and precipitation change individually. This supported hypothesis H_3. Specifically, the combined changes in temperature and precipitation caused ~~26~~24-~~35~~ 33 days per year (~~16~~15.~~1~~6-~~27~~26.~~4~~8%) increase in fire season length with the critical threshold of 79% LFMC under RCP 8.5 (Fig. 5). Under RCP 4.5, the combined changes in temperature and precipitation caused a ~~7~~6-~~10~~ 9 days per year (~~5~~4.~~0~~8-6.~~4~~1%) change in fire season length.

3.4 Comparison of changes in fire season length among three PFTs under climate change

Regarding three PFTs under both climate scenarios, fire season length of PFT-–H~~P~~A~~H~~ was the longest (~~165~~167-176 days per year), while fire season length of PFT-–M~~P~~C~~H~~ was the shortest (~~113~~114-124 per year) during ~~2075~~2080-2099 (Fig. 4). However, the response of fire season length to warming was strongest for PFT-–M~~P~~C~~H~~. Specifically, for PFT-–M~~P~~C~~H~~, warming under RCP 8.5 led to an increase of ~~23~~ 22 days in fire season length (Fig. 5 b) and warming under RCP 4.5 led to an increase of ~~12~~ 11 days in fire season length. For PFT~~-~~–L~~P~~A~~H~~, warming under RCP 8.5 led to an increase of ~~21~~ 19 days in fire season length (Fig. 5 a) while warming under RCP 4.5 led to an increase of ~~10~~ 9 days in fire season length. Finally, for PFT~~-~~–H~~P~~A~~H~~, warming under RCP 8.5 led to an increase of ~~19~~ 18 days in fire season length (Fig. 5 c) and ~~9~~ 8 days in fire season length with under RCP 4.5. Because PFT~~-~~–M~~P~~C~~H~~ has a more conservative hydraulic strategy with less negative P_{50}, turgor loss point and water potential at full turgor, this result supported hypothesis H_4 that the more conservative hydraulic strategy will be more vulnerable~~sensitive~~ to warming.

4. Discussion

Low LFMC within shrub leaves and ~~small branches~~shoots increases the flammability and likelihood of combustion, making it vitally important to monitor temporal variations in LFMC, especially during the dry season (Dennison et al, 2008). The strong relationships between observed and simulated LFMC of all PFTs suggested that the plant hydrodynamic model, FATES-HYDRO, could accurately estimate LFMC seasonal dynamics as a function of modeled leaf water content, and consequently be useful to predict fire risks in Mediterranean-type climate regions, although only small amount of validation data were used and the underlying assumption that a shrub was analogous to a small tree. During the future period (~~2075~~2080-2099) and the historical period (~~1950~~1960-1999), both periods displayed lower values in the dry season (April - October), which is consistent with lower LFMC during the summer-fall dry season, rather than the winter-spring wet season (Chuvieco et al, 2004; Pellizzaro et al, 2007; Pivovaroff et al. 2019). Extremely low daily LFMC was more likely to occur during the future period, which had higher temperature than the historical period. From the historical to the future period, fire season length could increase by 5.~~5~~2-~~15~~14.~~2~~8% ~~as determined by the critical threshold of LFMC of 79%~~

under climate change for chaparral shrub ecosystems (H_0). ~~Given that~~The fire season length was not validated, rather it was defined as number of days with LFMC below 79%.

Quantifying influences of climatic variables on LFMC is crucial to predicting future fire risks (Dennison & Moritz, 2009). Our results showed that future warming was the most important driver of LFMC while relative humidity was the least important driver. ~~.~~This finding suggested that warming~~higher temperature~~ would substantially push Vapor Pressure Deficit (VPD) higher and decrease LFMC and strongly increase the fire season length, which may greatly increase fire risks in the future (e.g. Dennison et al, 2008; Chuvieco et al, 2009; Pimont et al, 2019). Relative humidity would not strongly affect LFMC under climate change. CO_2 fertilization is expected to reduce stomatal conductance (Pataki et al. 2000; Tognetti et al. 2000) and thus could mitigate the impacts of warming on LFMC. Our results illustrated~~displayed~~ that, even though the CO_2 impact did cause a 3.~~7~~5-~~5~~4.~~1~~8% reduction in fire season length, the impact of warming on fire season length is about 5.~~8~~6-~~14~~13.8% larger than the CO_2 effect (H_1, warming has a stronger impact on LFMC than CO_2 fertilization). This result suggests that CO_2 fertilization cannot offset the LFMC impacts from warming. The FATES-HYDRO model assumes a consistent stomatal sensitivity to CO_2 concentration across Mediterranean shrub species. While Mediterranean shrub functional types ~~species~~ in arid and semi-arid systems would vary in their stomatal response in the real world (Pataki et al. 2000). Therefore, our model may overestimate/underestimate the CO_2 effect on stomatal conductance and its mitigating influence might be smaller in reality for some species.

Previous studies implied that the timing of precipitation may have a strong impact on subsequent LFMC (e.g. Veblen et al. 2000; Westerling et al. 2006; Dennison & Moritz 2009). In this study, precipitation was also ~~the~~ a key driver of LFMC under future climate conditions. Our results showed that, even though total precipitation was projected to increase, the reduction in spring and autumn precipitation (Fig. S2) was projected to cause a longer fire season length (H_2, the reductions in spring and autumn precipitation lead to a longer fire season as determined by LFMC; Fig. 5). This result was in agreement with a prior study indicating that spring precipitation, particularly in the month of March, was found to be the primary driver of timing of LFMC changes (Dennison & Moritz 2009). We also found that the combined impacts of warming and precipitation on fire season length were equal to the linearly additive impacts of warming and precipitation change individually (H_3). Our results suggested that, when evaluating future fire risks, it is critical that we considered the seasonal changes in precipitation and its interaction with the warming impact.

Modeled vegetation responses to environmental changes ~~could be~~is a function of variation in plant functional traits ~~determined by variations in traits~~ (Koven et al, 2020). ~~For~~ The three PFTs represented in this study have ~~co-occurred in the simulations, even though they grew together and showed~~ similar patterns in LFMC in response to climate change during ~~1950~~1960-2099, but we did see some critical differences. Specifically, the plant functional type ~~(~~PFT-–M~~P~~C~~H)~~ with more conservative hydraulic strategy had the strongest responses to climate change (Fig. 5). This could be related to the fact that the PFT-–M~~P~~C~~H~~ is a more conservative drought tolerant~~ce~~ PFT in terms of hydraulic strategy with less negative P_{50}, turgor loss point, and water potential at full turgor. The PFT-–M~~P~~C~~H~~ plants had a relatively high saturated water content based on observed data (Fig 2) and the water within plant tissues thus ~~could~~ changes more quickly in response to the environmental condition changes (H_4, plants with more conservative hydraulic strategies will be more vulnerable to warming). However, the three different PFTs were coexisting at the same location in model simulations, coexistence and heterogeneity in LFMC might impact fire behavior and fire season length.

Because the moisture content of live fuels (~50–200%) are much higher than that of dead fuels (~7–30%), leaf senescence induced by drought stress and subsequent mortality are potentially vital factors to cause large wildfires (Nolan et al. 2016, 2020). Thus drought-induced canopy die-back and mortality could largely increase surface fine fuel loads and vegetation flammability, which can increase the probability of wildfire (Ruthrof et al. 2016). Since growth and mortality are turned off in model runs by using a reduced-complexity configuration, it is possible that vegetation density might decrease and LFMC could be conserved under future scenarios. In addition, potential vegetation transitions (e.g., shrubs to grassland and species composition changes) might substantially affect flammability and thus fire intensity and frequency. In this study, we used the static mode of FATES-HYDRO to simulate LWC dynamics under climate change. If we need to assess how the leaf senescence and vegetation dynamics will impact the fire behavior, we can use the same model with dynamic mode to assess their impacts on fire behaviors under future drought and warming conditions.

Application of a hydrodynamic vegetation model to estimate LFMC dynamics could potentially benefit wildfire modeling at the fine-scale, landscape-scale, and global-scale. This is because LFMC is one of the most critical factors influencing combustion, fire spread, and fire consumption while previous wildfire models mainly focus on impacts of dead fuel moisture, weather conditions on wildfire, fuel loads, and representation of live fuel moisture (Anderson & Anderson 2010; Keeley et al. 2011; Jolly & Johnson 2018). -The implications of this are that fire potential will vary with plant water potential and uptake from soils, photosynthetic and respiratory activity, carbon allocation and phenology with variability across species and over time (Jolly & Johnson 2018). Therefore, future work to incorporate LFMC dynamics in wildfire models could potentially play a vitally important role in the future studies of wildfire modeling under climate change.

5. Conclusions

A hydrodynamic vegetation model, FATES-HYDRO, was used to estimate leaf water status and thus LFMC ~~historical and future LFMC~~ dynamics of chaparral shrub species in southern California under historical and future conditions~~climate change~~. FATES-HYDRO model was validated using monthly mean LFMC for three PFTs. The fire season length was projected to substantially increase under both climate scenarios from ~~1950~~1960-1999 to ~~2075~~2080-2099. This could increase wildlife risk over time for chaparral shrubs in southern California. Our results showed that temperature was the most important driver of LFMC and relative humidity was the least important among four climatic variables including CO_2, temperature, precipitation, and relative humidity. The LFMC estimated by the FATES-HYDRO model offered a baseline of predicting plant hydraulic dynamics subjected to climate change and provided a critical foundation that reductions in LFMC from climate warming may exacerbate future wildfire risk. Longer fire season might have a significant impact on overall public health and quality of life in the future.

Acknowledgements

This project is supported by the University of California Office of the President Lab Fees Research Program and the Next Generation Ecosystem Experiment (NGEE) Tropics, which is supported by the U.S. DOE Office of Science. CDK and JD are supported by the DOE Office of Science, Regional and Global Model Analysis Program, Early Career Research Program. R

statistical software is applied to make figures for this study. A repository link for FATES is https://github.com/xuchongang/fates.

References

Abatzoglou, J.T. and Brown, T.J., 2012. A comparison of statistical downscaling methods suited for wildfire applications. *International Journal of Climatology*, *32*(5), pp.772-780.

Abatzoglou JT (2013) Development of gridded surface meteorological data for ecological applications and modelling. *International Journal of Climatology*, 33, 121-131.

Agee, J.K., Wright, C.S., Williamson, N. and Huff, M.H., 2002. Foliar moisture content of Pacific Northwest vegetation and its relation to wildland fire behavior. *Forest ecology and management*, *167*(1-3), pp.57-66.

Anderson, S.A. and Anderson, W.R., 2010. Ignition and fire spread thresholds in gorse (Ulex europaeus). *International Journal of Wildland Fire*, *19*(5), pp.589-598.

Aguado, I., Chuvieco, E., Boren, R. and Nieto, H., 2007. Estimation of dead fuel moisture content from meteorological data in Mediterranean areas. Applications in fire danger assessment. *International Journal of Wildland Fire*, *16*(4), pp.390-397.

Bistinas, I., Harrison, S.P., Prentice, I.C. and Pereira, J.M.C., 2014. Causal relationships versus emergent patterns in the global controls of fire frequency. *Biogeosciences*, *11*(18), pp.5087-5101.

Burgan, R.E. Estimating Live Fuel Moisture for the 1978 National Fire Danger Rating System; Intermountain Forest and Range Experiment Station: Ogden, UT, USA, 1979.

Bilgili, E. and Saglam, B., 2003. Fire behavior in maquis fuels in Turkey. *Forest Ecology and Management*, *184*(1-3), pp.201-207.

Balch, J.K., Bradley, B.A., Abatzoglou, J.T., Nagy, R.C., Fusco, E.J. and Mahood, A.L., 2017. Human-started wildfires expand the fire niche across the United States. *Proceedings of the National Academy of Sciences*, *114*(11), pp.2946-2951.

Bartlett, M.K., Scoffoni, C. and Sack, L., 2012. The determinants of leaf turgor loss point and prediction of drought tolerance of species and biomes: a global meta-analysis. *Ecology letters*, *15*(5), pp.393-405.

Bridges Jr, C.C., 1966. Hierarchical cluster analysis. *Psychological reports*, *18*(3), pp.851-854.

Christoffersen, B.O., Gloor, M., Fauset, S., Fyllas, N.M., Galbraith, D.R., Baker, T.R., Kruijt, B., Rowland, L., Fisher, R.A., Binks, O.J. and Sevanto, S., 2016. Linking hydraulic traits to tropical forest function in a size-structured and trait-driven model (TFS v. 1-Hydro). Geoscientific Model Development. 9: 4227-4255.

Caccamo, G., Chisholm, L.A., Bradstock, R.A. and Puotinen, M.L., 2012a. Using remotely-sensed fuel connectivity patterns as a tool for fire danger monitoring. *Geophysical Research Letters*, *39*(1).

Caccamo, G., Chisholm, L.A., Bradstock, R.A., Puotinen, M.L. and Pippen, B.G., 2012b. Monitoring live fuel moisture content of heathland, shrubland and sclerophyll forest in south-eastern Australia using MODIS data. *International Journal of Wildland Fire*, *21*(3), pp.257-269.

Clarke, H., Pitman, A.J., Kala, J., Carouge, C., Haverd, V. and Evans, J.P., 2016. An investigation of future fuel load and fire weather in Australia. *Climatic Change*, *139*(3-4), pp.591-605.

Chuvieco, E., Cocero, D., Riano, D., Martin, P., Martınez-Vega, J., de la Riva, J. and Pérez, F., 2004. Combining NDVI and surface temperature for the estimation of live fuel moisture content in forest fire danger rating. Remote Sensing of Environment, 92(3), pp.322-331.

Caldwell, P.M., Mametjanov, A., Tang, Q., Van Roekel, L.P., Golaz, J.C., Lin, W., Bader, D.C., Keen, N.D., Feng, Y., Jacob, R. and Maltrud, M.E., 2019. The DOE E3SM coupled model version 1: Description and results at high resolution. *Journal of Advances in Modeling Earth Systems*, *11*(12), pp.4095-4146.

Castro, F.X., Tudela, A. and Sebastià, M.T., 2003. Modeling moisture content in shrubs to predict fire risk in Catalonia (Spain). *Agricultural and Forest Meteorology*, *116*(1-2), pp.49-59.

Chuvieco, E., González, I., Verdú, F., Aguado, I. and Yebra, M., 2009. Prediction of fire occurrence from live fuel moisture content measurements in a Mediterranean ecosystem. *International Journal of Wildland Fire*, *18*(4), pp.430-441.

Collins, M., Knutti, R., Arblaster, J., Dufresne, J.L., Fichefet, T., Friedlingstein, P., Gao, X., Gutowski, W.J., Johns, T., Krinner, G. and Shongwe, M., 2013. Long-term climate change: projections, commitments and irreversibility. In *Climate Change 2013-The Physical Science Basis: Contribution of Working Group I to the Fifth Assessment Report of the Intergovernmental Panel on Climate Change* (pp. 1029-1136). Cambridge University Press.

Cook, B.I., Smerdon, J.E., Seager, R. and Coats, S., 2014. Global warming and 21 st century drying. *Climate Dynamics*, *43*(9-10), pp.2607-2627.

Dennison, P.E., Moritz, M.A. and Taylor, R.S., 2008. Evaluating predictive models of critical live fuel moisture in the Santa Monica Mountains, California. *International Journal of Wildland Fire*, *17*(1), pp.18-27.

Dennison, P.E. and Moritz, M.A., 2009. Critical live fuel moisture in chaparral ecosystems: a threshold for fire activity and its relationship to antecedent precipitation. *International Journal of Wildland Fire*, *18*(8), pp.1021-1027.

Dimitrakopoulos, A.P. and Papaioannou, K.K., 2001. Flammability assessment of Mediterranean forest fuels. *Fire Technology*, *37*(2), pp.143-152.

Dai, A., 2013. Increasing drought under global warming in observations and models. *Nature climate change*, *3*(1), pp.52-58.

Duursma, R.A. and Medlyn, B.E., 2012. MAESPA: a model to study interactions between water limitation, environmental drivers and vegetation function at tree and stand levels, with an example application to [CO_2]×drought interactions.

Flannigan, M.D., Krawchuk, M.A., de Groot, W.J., Wotton, B.M. and Gowman, L.M., 2009. Implications of changing climate for global wildland fire. *International journal of wildland fire*, *18*(5), pp.483-507.

Fisher, R.A., Williams, M., Da Costa, A.L., Malhi, Y., Da Costa, R.F., Almeida, S. and Meir, P., 2007. The response of an Eastern Amazonian rain forest to drought stress: results and modelling analyses from a throughfall exclusion experiment. *Global Change Biology*, *13*(11), pp.2361-2378.

Fisher, R.A., Muszala, S., Verteinstein, M., Lawrence, P., Xu, C., McDowell, N.G., Knox, R.G., Koven, C., Holm, J., Rogers, B.M. and Spessa, A., 2015. Taking off the training wheels: the properties of a dynamic vegetation model without climate envelopes, CLM4. 5 (ED). *Geoscientific Model Development*, *8*(11), pp.3593-3619.

Fisher, R.A., Koven, C.D., Anderegg, W.R., Christoffersen, B.O., Dietze, M.C., Farrior, C.E., Holm, J.A., Hurtt, G.C., Knox, R.G., Lawrence, P.J. and Lichstein, J.W., 2018. Vegetation demographics in Earth System Models: A review of progress and priorities. *Global change biology*, *24*(1), pp.35-54.

Gillett, N.P., Weaver, A.J., Zwiers, F.W. and Flannigan, M.D., 2004. Detecting the effect of climate change on Canadian forest fires. *Geophysical Research Letters*, *31*(18).

Goss, M., Swain, D.L., Abatzoglou, J.T., Sarhadi, A., Kolden, C.A., Williams, A.P. and Diffenbaugh, N.S., 2020. Climate change is increasing the likelihood of extreme autumn wildfire conditions across California. *Environmental Research Letters*, *15*(9), p.094016.

Hantson, S., Arneth, A., Harrison, S.P., Kelley, D.I., Prentice, I.C., Rabin, S.S., Archibald, S., Mouillot, F., Arnold, S.R., Artaxo, P. and Bachelet, D., 2016. The status and challenge of global fire modelling. *Biogeosciences*, *13*(11), pp.3359-3375.

Holm, J.A., Shugart, H.H., Van Bloem, S.J. and Larocque, G.R., 2012. Gap model development, validation, and application to succession of secondary subtropical dry forests of Puerto Rico. *Ecological Modelling*, *233*, pp.70-82.

Jacobsen, A. L., Pratt, R. B., Davis, S. D., & Ewers, F. W. (2008). Comparative community physiology: nonconvergence in water relations among three semi-arid shrub communities. New Phytologist, 180(1), 100-113.

Jolly, W.M. and Johnson, D.M., 2018. Pyro-ecophysiology: shifting the paradigm of live wildland fuel research. *Fire*, *1*(1), p.8.

Jackson, D.A., 1993. Stopping rules in principal components analysis: a comparison of heuristical and statistical approaches. *Ecology*, *74*(8), pp.2204-2214.

Kelley, D.I., Bistinas, I., Whitley, R., Burton, C., Marthews, T.R. and Dong, N., 2019. How contemporary bioclimatic and human controls change global fire regimes. *Nature Climate Change*, *9*(9), pp.690-696.

Konings, A.G., Rao, K. and Steele-Dunne, S.C., 2019. Macro to micro: microwave remote sensing of plant water content for physiology and ecology. *New Phytologist*, *223*(3), pp.1166-1172.

Keeley, J.E., 1995. Future of California floristics and systematics: wildfire threats to the California flora. Madrono, pp.175-179.

Keeley, J.E. and Zedler, P.H., 2009. Large, high-intensity fire events in southern California shrublands: debunking the fine-grain age patch model. *Ecological Applications*, *19*(1), pp.69-94.

Keeley, J.E., Bond, W.J., Bradstock, R.A., Pausas, J.G. and Rundel, P.W., 2011. *Fire in Mediterranean ecosystems: ecology, evolution and management*. Cambridge University Press.

Kennedy, D., Swenson, S., Oleson, K.W., Lawrence, D.M., Fisher, R., Lola da Costa, A.C. and Gentine, P., 2019. Implementing plant hydraulics in the community land model, version 5. *Journal of Advances in Modeling Earth Systems*, *11*(2), pp.485-513.

Koven, C.D., Knox, R.G., Fisher, R.A., Chambers, J.Q., Christoffersen, B.O., Davies, S.J., Detto, M., Dietze, M.C., Faybishenko, B., Holm, J. and Huang, M., 2020. Benchmarking and parameter sensitivity of physiological and vegetation dynamics using the Functionally

Assembled Terrestrial Ecosystem Simulator (FATES) at Barro Colorado Island, Panama. *Biogeosciences*, *17*(11), pp.3017-3044.

Krawchuk, M.A., Moritz, M.A., Parisien, M.A., Van Dorn, J. and Hayhoe, K., 2009. Global pyrogeography: the current and future distribution of wildfire. *PloS one*, *4*(4), p.e5102.

Linn, R., Reisner, J., Colman, J.J. and Winterkamp, J., 2002. Studying wildfire behavior using FIRETEC. *International journal of wildland fire*, *11*(4), pp.233-246.

Liu, Y., Stanturf, J. and Goodrick, S., 2010. Trends in global wildfire potential in a changing climate. *Forest ecology and management*, *259*(4), pp.685-697.

Massoud, E.C., Xu, C., Fisher, R.A., Knox, R.G., Walker, A.P., Serbin, S.P., Christoffersen, B.O., Holm, J.A., Kueppers, L.M., Ricciuto, D.M. and Wei, L., 2019. Identification of key parameters controlling demographically structured vegetation dynamics in a land surface model: CLM4. 5 (FATES). *Geoscientific Model Development*, *12*(9), pp.4133-4164.

Moorcroft, P.R., Hurtt, G.C. and Pacala, S.W., 2001. A method for scaling vegetation dynamics: the ecosystem demography model (ED). *Ecological monographs*, *71*(4), pp.557-586.

Mikkelsen, T.N., Beier, C., Jonasson, S., Holmstrup, M., Schmidt, I.K., Ambus, P., Pilegaard, K., Michelsen, A., Albert, K., Andresen, L.C. and Arndal, M.F., 2008. Experimental design of multifactor climate change experiments with elevated CO2, warming and drought: the CLIMAITE project. *Functional Ecology*, *22*(1), pp.185-195.

Moritz, M.A., Parisien, M.A., Batllori, E., Krawchuk, M.A., Van Dorn, J., Ganz, D.J. and Hayhoe, K., 2012. Climate change and disruptions to global fire activity. *Ecosphere*, *3*(6), pp.1-22.

McDowell, N.G., Fisher, R.A., Xu, C., Domec, J.C., Hölttä, T., Mackay, D.S., Sperry, J.S., Boutz, A., Dickman, L., Gehres, N. and Limousin, J.M., 2013. Evaluating theories of drought-induced vegetation mortality using a multimodel–experiment framework. *New Phytologist*, *200*(2), pp.304-321.

Mencuccini, M., Manzoni, S. and Christoffersen, B., 2019. Modelling water fluxes in plants: from tissues to biosphere. *New Phytologist*, *222*(3), pp.1207-1222.

Matthews, S., Sullivan, A.L., Watson, P. and Williams, R.J., 2012. Climate change, fuel and fire behaviour in a eucalypt forest. *Global Change Biology*, *18*(10), pp.3212-3223.

Manabe, S. and Wetherald, R.T., 1975. The effects of doubling the CO2 concentration on the climate of a general circulation model. *Journal of the Atmospheric Sciences*, *32*(1), pp.3-15.

Meinzer, F.C., James, S.A., Goldstein, G. and Woodruff, D., 2003. Whole-tree water transport scales with sapwood capacitance in tropical forest canopy trees. *Plant, Cell & Environment*, *26*(7), pp.1147-1155.

Meinzer, F.C., Johnson, D.M., Lachenbruch, B., McCulloh, K.A. and Woodruff, D.R., 2009. Xylem hydraulic safety margins in woody plants: coordination of stomatal control of xylem tension with hydraulic capacitance. *Functional Ecology*, *23*(5), pp.922-930.

Meinshausen, M., Smith, S.J., Calvin, K., Daniel, J.S., Kainuma, M.L., Lamarque, J.F., Matsumoto, K., Montzka, S.A., Raper, S.C., Riahi, K. and Thomson, A.G.J.M.V., 2011. The RCP greenhouse gas concentrations and their extensions from 1765 to 2300. *Climatic change*, *109*(1), pp.213-241.

Nolan, R.H., Boer, M.M., Resco de Dios, V., Caccamo, G. and Bradstock, R.A., 2016. Large-scale, dynamic transformations in fuel moisture drive wildfire activity across southeastern Australia. *Geophysical Research Letters*, *43*(9), pp.4229-4238.

Nolan, R.H., Blackman, C.J., de Dios, V.R., Choat, B., Medlyn, B.E., Li, X., Bradstock, R.A. and Boer, M.M., 2020. Linking forest flammability and plant vulnerability to drought. *Forests*, *11*(7), p.779.

Pivovaroff, A. L., Emery, N., Sharifi, M. R., Witter, M., Keeley, J. E., & Rundel, P. W. (2019). The effect of ecophysiological traits on live fuel moisture content. Fire, 2(2), 28.

Powell, T.L., Koven, C.D., Johnson, D.J., Faybishenko, B., Fisher, R.A., Knox, R.G., McDowell, N.G., Condit, R., Hubbell, S.P., Wright, S.J. and Chambers, J.Q., 2018. Variation in hydroclimate sustains tropical forest biomass and promotes functional diversity. *New Phytologist*, *219*(3), pp.932-946.

Pellizzaro, G., Cesaraccio, C., Duce, P., Ventura, A. and Zara, P., 2007. Relationships between seasonal patterns of live fuel moisture and meteorological drought indices for Mediterranean shrubland species. *International Journal of Wildland Fire*, *16*(2), pp.232-241.

Plucinski, M.P., 2003. The investigation of factors governing ignition and development of fires in heathland vegetation. *PhD thesis. University of New South Wales, Sydney*.

Pimont, F., Ruffault, J., Martin-StPaul, N.K. and Dupuy, J.L., 2019. Why is the effect of live fuel moisture content on fire rate of spread underestimated in field experiments in shrublands?. *International journal of wildland fire*, *28*(2), pp.127-137.

Pataki, D.E., Huxman, T.E., Jordan, D.N., Zitzer, S.F., Coleman, J.S., Smith, S.D., Nowak, R.S. and Seemann, J.R., 2000. Water use of two Mojave Desert shrubs under elevated CO2. *Global Change Biology*, *6*(8), pp.889-897.

Pineda-Garcia, F., Paz, H. and Meinzer, F.C., 2013. Drought resistance in early and late secondary successional species from a tropical dry forest: the interplay between xylem resistance to embolism, sapwood water storage and leaf shedding. *Plant, Cell & Environment*, *36*(2), pp.405-418.

Rabin, S.S., Melton, J.R., Lasslop, G., Bachelet, D., Forrest, M., Hantson, S., Kaplan, J.O., Li, F., Mangeon, S., Ward, D.S. and Yue, C., 2017. The Fire Modeling Intercomparison Project (FireMIP), phase 1: experimental and analytical protocols with detailed model descriptions. *Geoscientific Model Development*, *10*(3), pp.1175-1197.

Rossa, C.G. and Fernandes, P.M., 2018. Live fuel moisture content: The 'pea under the mattress' of fire spread rate modeling?. *Fire*, *1*(3), p.43.

Rind, D., Goldberg, R., Hansen, J., Rosenzweig, C. and Ruedy, R., 1990. Potential evapotranspiration and the likelihood of future drought. *Journal of Geophysical Research: Atmospheres*, *95*(D7), pp.9983-10004.

Rothermel, R.C., 1972. *A mathematical model for predicting fire spread in wildland fuels* (Vol. 115). Intermountain Forest & Range Experiment Station, Forest Service, US Department of Agriculture.

Ruthrof, K.X., Fontaine, J.B., Matusick, G., Breshears, D.D., Law, D.J., Powell, S. and Hardy, G., 2016. How drought-induced forest die-off alters microclimate and increases fuel loadings and fire potentials. *International Journal of Wildland Fire*, *25*(8), pp.819-830.

Sturtevant, B.R., Scheller, R.M., Miranda, B.R., Shinneman, D. and Syphard, A., 2009. Simulating dynamic and mixed-severity fire regimes: a process-based fire extension for LANDIS-II. *Ecological Modelling*, *220*(23), pp.3380-3393.

Stocks, B.J., Fosberg, M.A., Lynham, T.J., Mearns, L., Wotton, B.M., Yang, Q., Jin, J.Z., Lawrence, K., Hartley, G.R., Mason, J.A. and McKenney, D.W., 1998. Climate change and forest fire potential in Russian and Canadian boreal forests. *Climatic change*, *38*(1), pp.1-13.

Schroeder, M.J., Glovinsky, M., Henricks, V.F., Hood, F.C. and Hull, M.K., 1964. *Synoptic weather types associated with critical fire weather*. USDA Forest Service, Pacific Southwest Range and Experiment Station. Berkeley, CA.

Seiler, C., Hutjes, R.W.A., Kruijt, B., Quispe, J., Añez, S., Arora, V.K., Melton, J.R., Hickler, T. and Kabat, P., 2014. Modeling forest dynamics along climate gradients in Bolivia. *Journal of Geophysical Research: Biogeosciences*, *119*(5), pp.758-775.

Sheffield, J. and Wood, E.F., 2008. Projected changes in drought occurrence under future global warming from multi-model, multi-scenario, IPCC AR4 simulations. *Climate dynamics*, *31*(1), pp.79-105.

Saura-Mas, S. and Lloret, F., 2007. Leaf and shoot water content and leaf dry matter content of Mediterranean woody species with different post-fire regenerative strategies. *Annals of Botany*, *99*(3), pp.545-554.

Thonicke, K., Spessa, A., Prentice, I.C., Harrison, S.P., Dong, L. and Carmona-Moreno, C., 2010. The influence of vegetation, fire spread and fire behaviour on biomass burning and trace gas emissions: results from a process-based model. *Biogeosciences*, *7*(6), pp.1991-2011.

Tyree, M.T. and Hammel, H.T., 1972. The measurement of the turgor pressure and the water relations of plants by the pressure-bomb technique. *Journal of experimental Botany*, *23*(1), pp.267-282.

Tyree, M.T. and Yang, S., 1990. Water-storage capacity of Thuja, Tsuga and Acer stems measured by dehydration isotherms. *Planta*, *182*(3), pp.420-426.

Tognetti, R., Minnocci, A., Peñuelas, J., Raschi, A. and Jones, M.B., 2000. Comparative field water relations of three Mediterranean shrub species co-occurring at a natural CO2 vent. *Journal of Experimental Botany*, *51*(347), pp.1135-1146.

Tjiputra, J.F., Roelandt, C., Bentsen, M., Lawrence, D.M., Lorentzen, T., Schwinger, J., Seland, Ø. and Heinze, C., 2013. Evaluation of the carbon cycle components in the Norwegian Earth System Model (NorESM). *Geoscientific Model Development*, *6*(2), pp.301-325.

Venturas, M. D., MacKinnon, E. D., Dario, H. L., Jacobsen, A. L., Pratt, R. B., & Davis, S. D. (2016). Chaparral shrub hydraulic traits, size, and life history types relate to species mortality during California's historic drought of 2014. PLOS One, 11(7).

Veblen, T.T., Kitzberger, T. and Donnegan, J., 2000. Climatic and human influences on fire regimes in ponderosa pine forests in the Colorado Front Range. *Ecological applications*, *10*(4), pp.1178-1195.

Westerling, A.L., Gershunov, A., Brown, T.J., Cayan, D.R. and Dettinger, M.D., 2003. Climate and wildfire in the western United States. *Bulletin of the American Meteorological Society*, *84*(5), pp.595-604.

Westerling, A.L., Hidalgo, H.G., Cayan, D.R. and Swetnam, T.W., 2006. Warming and earlier spring increase western US forest wildfire activity. *science*, *313*(5789), pp.940-943.

Williams, A.P., Abatzoglou, J.T., Gershunov, A., Guzman-Morales, J., Bishop, D.A., Balch, J.K. and Lettenmaier, D.P., 2019. Observed impacts of anthropogenic climate change on wildfire in California. *Earth's Future*, *7*(8), pp.892-910.

Wullschleger, S.D., Gunderson, C.A., Hanson, P.J., Wilson, K.B. and Norby, R.J., 2002. Sensitivity of stomatal and canopy conductance to elevated CO2 concentration–interacting variables and perspectives of scale. *New Phytologist*, *153*(3), pp.485-496.

Wu, J., Serbin, S.P., Ely, K.S., Wolfe, B.T., Dickman, L.T., Grossiord, C., Michaletz, S.T., Collins, A.D., Detto, M., McDowell, N.G. and Wright, S.J., 2020. The response of stomatal conductance to seasonal drought in tropical forests. *Global Change Biology*, *26*(2), pp.823-839.

Wei, L., Xu, C., Jansen, S., Zhou, H., Christoffersen, B.O., Pockman, W.T., Middleton, R.S., Marshall, J.D. and McDowell, N.G., 2019. A heuristic classification of woody plants based on contrasting shade and drought strategies. *Tree physiology*, *39*(5), pp.767-781.

Xu, C., McDowell, N.G., Sevanto, S. and Fisher, R.A., 2013. Our limited ability to predict vegetation dynamics under water stress. *New Phytologist*, *200*(2), pp.298-300.

Xu, X., Medvigy, D., Powers, J.S., Becknell, J.M. and Guan, K., 2016. Diversity in plant hydraulic traits explains seasonal and inter-annual variations of vegetation dynamics in seasonally dry tropical forests. *New Phytologist*, *212*(1), pp.80-95.

Xu, C., McDowell, N.G., Fisher, R.A., Wei, L., Sevanto, S., Christoffersen, B.O., Weng, E. and Middleton, R.S., 2019. Increasing impacts of extreme droughts on vegetation productivity under climate change. *Nature Climate Change*, *9*(12), pp.948-953.

Yebra, M., Chuvieco, E. and Riaño, D., 2008. Estimation of live fuel moisture content from MODIS images for fire risk assessment. *Agricultural and forest meteorology*, *148*(4), pp.523-536.

Yebra, M., Dennison, P.E., Chuvieco, E., Riano, D., Zylstra, P., Hunt Jr, E.R., Danson, F.M., Qi, Y. and Jurdao, S., 2013. A global review of remote sensing of live fuel moisture content for fire danger assessment: Moving towards operational products. *Remote Sensing of Environment*, *136*, pp.455-468.

Yebra, M., Quan, X., Riaño, D., Larraondo, P.R., van Dijk, A.I. and Cary, G.J., 2018. A fuel moisture content and flammability monitoring methodology for continental Australia based on optical remote sensing. *Remote Sensing of Environment*, *212*, pp.260-272.

Zarco-Tejada, P.J., Rueda, C.A. and Ustin, S.L., 2003. Water content estimation in vegetation with MODIS reflectance data and model inversion methods. *Remote Sensing of Environment*, *85*(1), pp.109-124.

Zhao, T. and Dai, A., 2015. The magnitude and causes of global drought changes in the twenty-first century under a low–moderate emissions scenario. *Journal of climate*, *28*(11), pp.4490-4512.

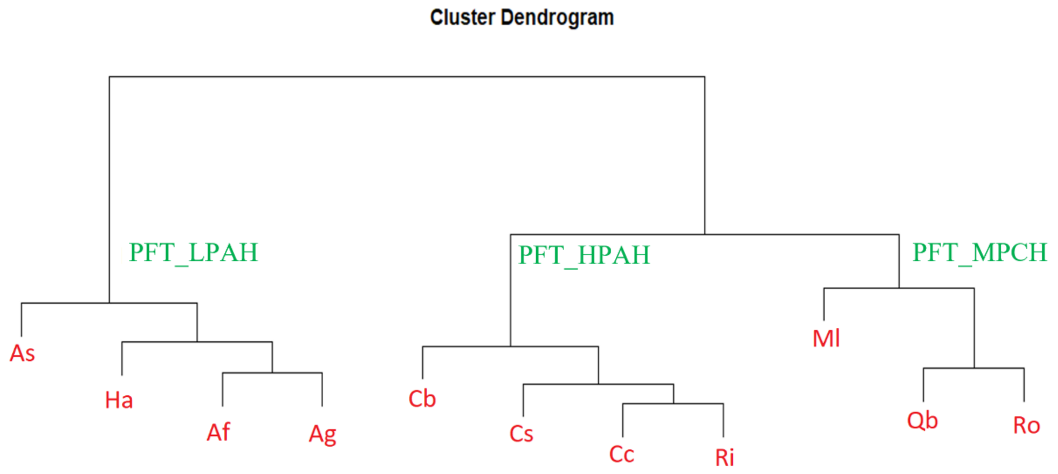

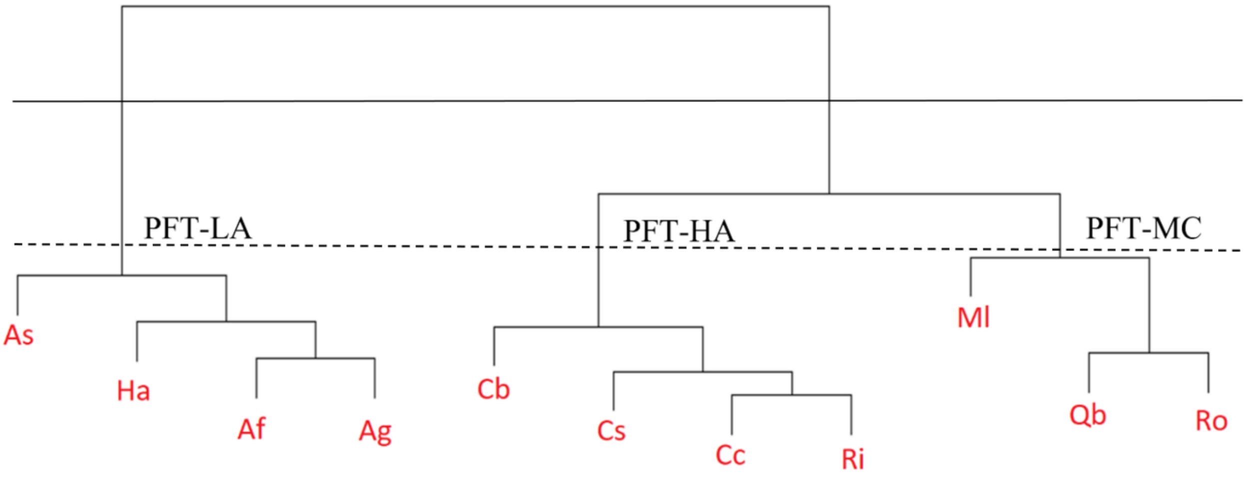

Fig 1. Hierarchical cluster analysis of allometry and hydraulic traits for eleven chaparral shrub species used to define three plant functional types at Stunt Ranch. The plant functional types with a ~~Low~~ low ~~Productivity~~ productivity and an ~~Aggressive~~ aggressive drought tolerance ~~Hydraulic~~ hydraulic strategy (PFT~~_~~-L~~P~~A~~H~~) was defined based on traits of red shank (Adenostoma sparsifolium - As), toyon (Heteromeles arbutifolia - Ha), Chamise (Adenostoma fasciculatum - Af), big berry manzanita (Arctostaphylos glauca - Ag); the plant functional types with a ~~High~~ high ~~Productivity~~ productivity and an ~~Aggressive~~ aggressive drought tolerance ~~Hydraulic~~ hydraulic strategy (PFT~~_~~-H~~P~~A~~H~~) was defined based on traits of mountain mahogany (Cercocarpus betuloides - Cb), greenbark ceanothus (Ceanothus spinosus - Cs), buck brush (Ceanothus cuneatus - Cc), hollyleaf redberry (Rhamnus ilicifolia - Ri); the plant functional types with a ~~Medium~~ medium ~~Productivity~~ productivity and an ~~Conservative~~ conservative ~~Hydraulic~~ drought tolerance hydraulic strategy (PFT~~_~~-M~~P~~C~~H~~) was defined based on traits of laurel sumac (Malosma laurina - Ml), scrub oak (Quercus berberidifolia - Qb), sugar bush (Rhus ovata - Ro).

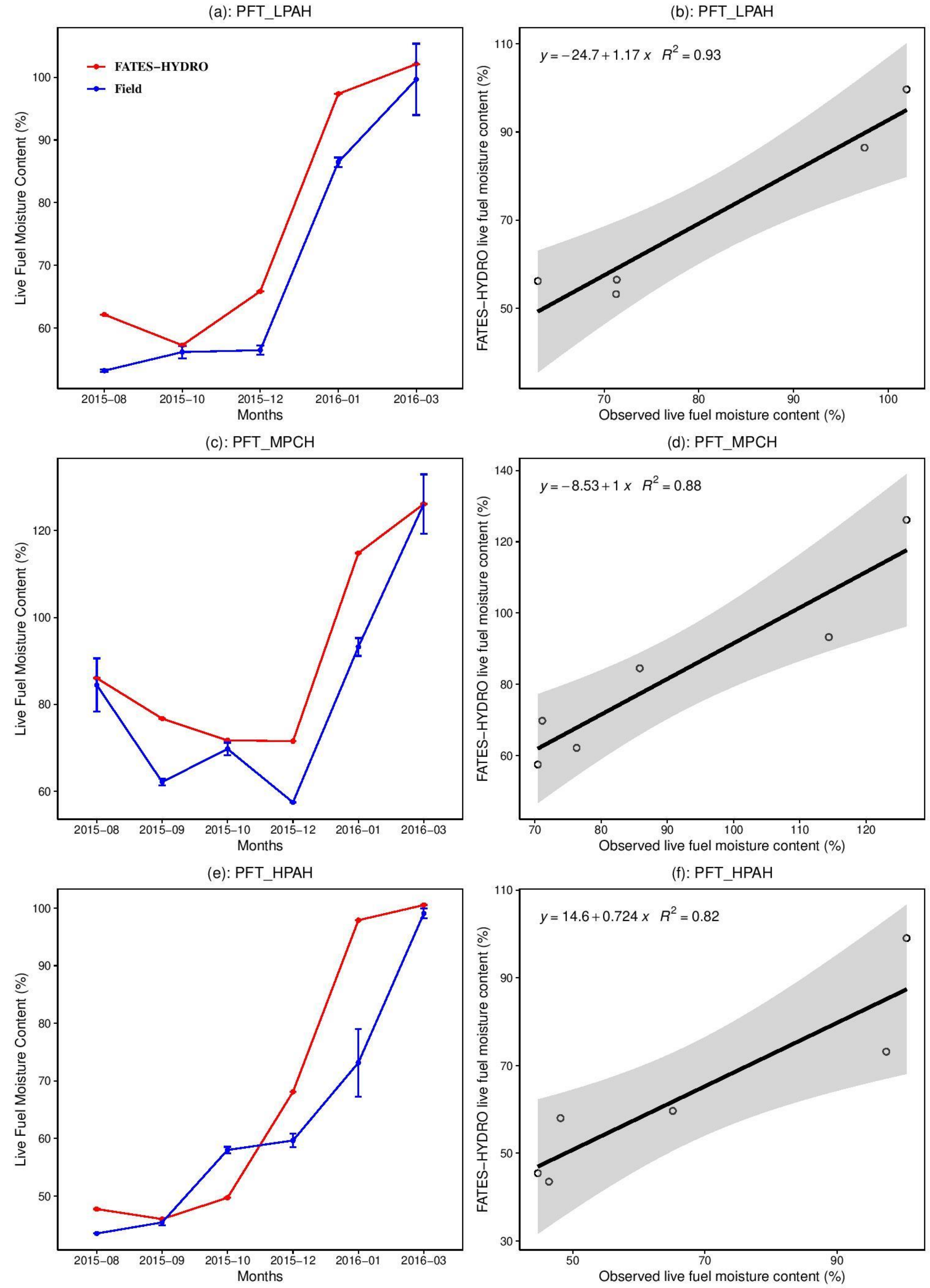
(a): PFT_LPAH
FATES−HYDRO
Field
Live Fuel Moisture Content (%)
60
70
80
90
100
2015−08
2015−10
2015−12
2016−01
2016−03
Months
(b): PFT_LPAH
$y = -24.7 + 1.17\ x\quad R^2 = 0.93$
FATES−HYDRO live fuel moisture content (%)
50
70
90
110
70
80
90
100
Observed live fuel moisture content (%)
(c): PFT_MPCH
Live Fuel Moisture Content (%)
60
80
100
120
2015−08
2015−09
2015−10
2015−12
2016−01
2016−03
Months
(d): PFT_MPCH
$y = -8.53 + 1\ x\quad R^2 = 0.88$
FATES−HYDRO live fuel moisture content (%)
60
80
100
120
140
70
80
90
100
110
120
Observed live fuel moisture content (%)
(e): PFT_HPAH
Live Fuel Moisture Content (%)
50
60
70
80
90
100
2015−08
2015−09
2015−10
2015−12
2016−01
2016−03
Months
(f): PFT_HPAH
$y = 14.6 + 0.724\ x\quad R^2 = 0.82$
FATES−HYDRO live fuel moisture content (%)
30
50
70
90
110
50
70
90
Observed live fuel moisture content (%)

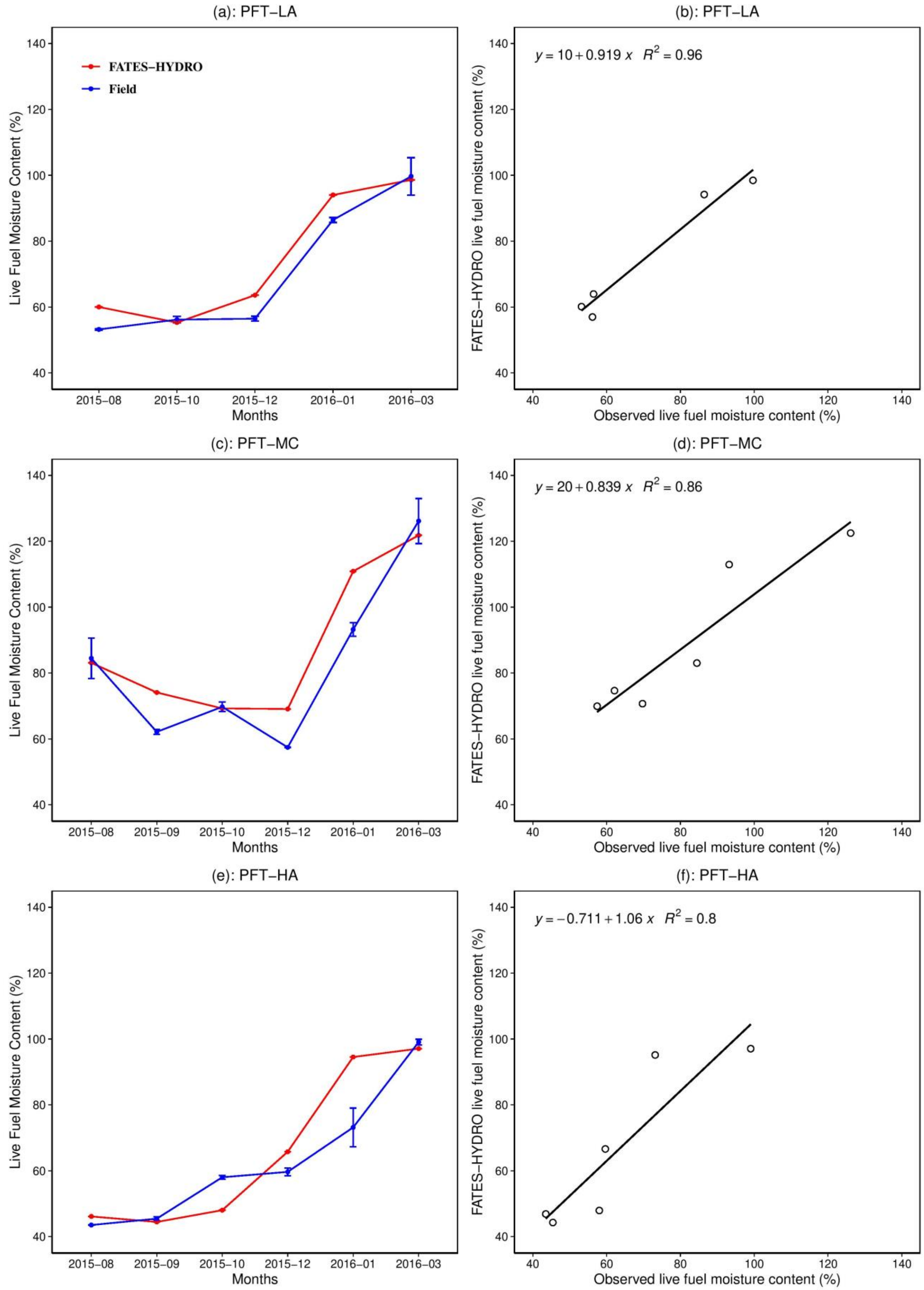

Fig.2 Simulated and observed monthly live fuel moisture content and related R^2 values for three PFTs (refer to Figure 1 for explanation of the PFTs).

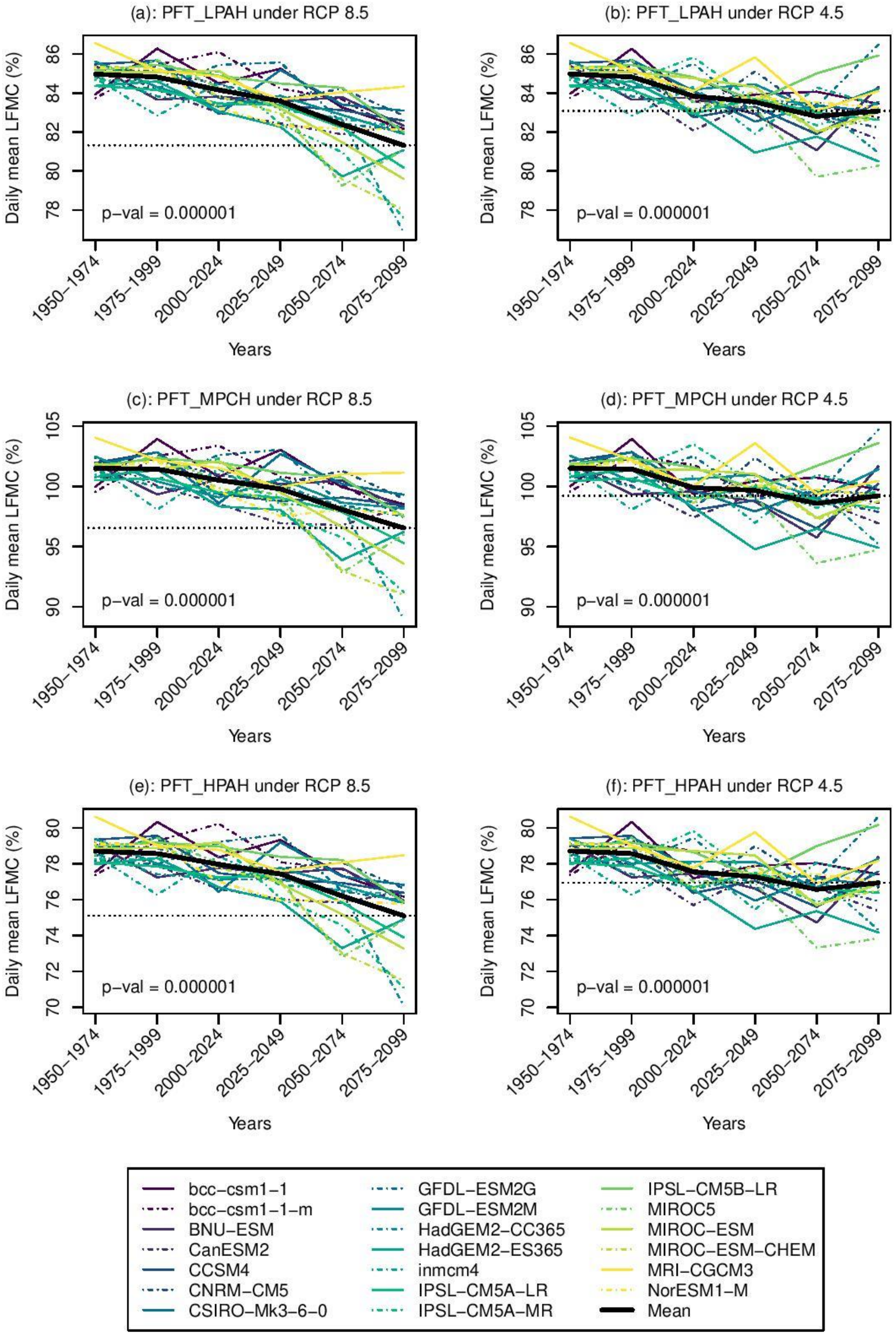
(a): PFT_LPAH under RCP 8.5
(b): PFT_LPAH under RCP 4.5
(c): PFT_MPCH under RCP 8.5
(d): PFT_MPCH under RCP 4.5
(e): PFT_HPAH under RCP 8.5
(f): PFT_HPAH under RCP 4.5
Daily mean LFMC (%)
Years
p−val = 0.000001
78
80
82
84
86
90
95
100
105
70
72
74
76
78
80
1950–1974
1975–1999
2000–2024
2025–2049
2050–2074
2075–2099
bcc−csm1−1
bcc−csm1−1−m
BNU−ESM
CanESM2
CCSM4
CNRM−CM5
CSIRO−Mk3−6−0
GFDL−ESM2G
GFDL−ESM2M
HadGEM2−CC365
HadGEM2−ES365
inmcm4
IPSL−CM5A−LR
IPSL−CM5A−MR
IPSL−CM5B−LR
MIROC5
MIROC−ESM
MIROC−ESM−CHEM
MRI−CGCM3
NorESM1−M
Mean

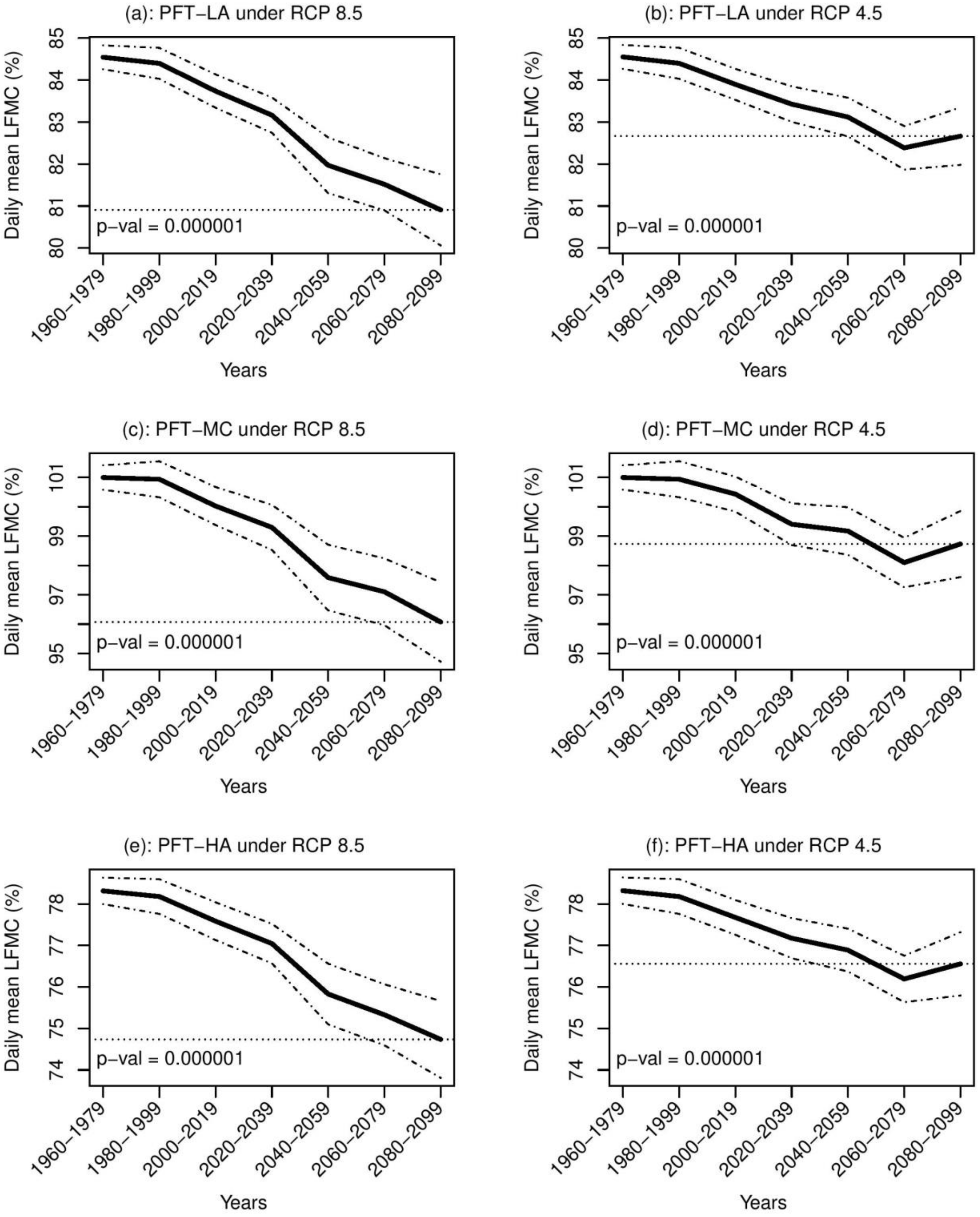

Fig.3 Temporal changes in daily mean live fuel moisture content (black solid line) and 95% confidence interval (black dash-dot line) from ~~1950~~ 1960 to 2099 for three PFTs (refer to Figure 1 for explanation of the PFTs) under climate scenario RCP 4.5 and 8.5 with 20 Earth System Models considering all climatic variables changes. The P values were calculated using bootstrap sampling to test whether the daily mean live fuel moisture content across different models during

the future period (~~2075~~2080–2099) was significantly lower than that during the historical period (~~1950~~1960-1999). The grey horizontal dotted line represents the ensemble mean for ~~2075~~2080–2099.

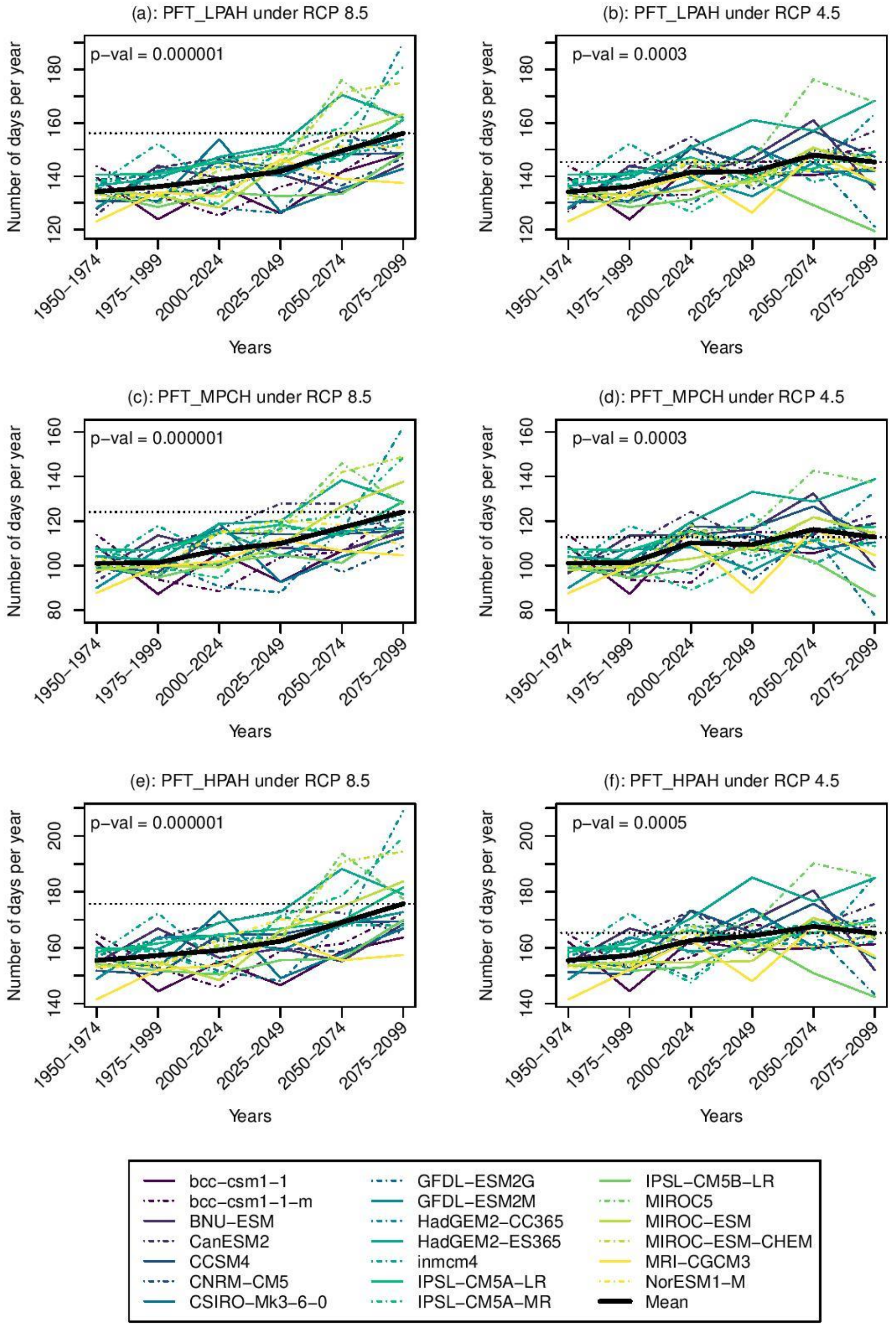
(a): PFT_LPAH under RCP 8.5
p−val = 0.000001
(b): PFT_LPAH under RCP 4.5
p−val = 0.0003
(c): PFT_MPCH under RCP 8.5
p−val = 0.000001
(d): PFT_MPCH under RCP 4.5
p−val = 0.0003
(e): PFT_HPAH under RCP 8.5
p−val = 0.000001
(f): PFT_HPAH under RCP 4.5
p−val = 0.0005
Number of days per year
Years
1950−1974
1975−1999
2000−2024
2025−2049
2050−2074
2075−2099
120
140
160
180
80
100
200
bcc−csm1−1
bcc−csm1−1−m
BNU−ESM
CanESM2
CCSM4
CNRM−CM5
CSIRO−Mk3−6−0
GFDL−ESM2G
GFDL−ESM2M
HadGEM2−CC365
HadGEM2−ES365
inmcm4
IPSL−CM5A−LR
IPSL−CM5A−MR
IPSL−CM5B−LR
MIROC5
MIROC−ESM
MIROC−ESM−CHEM
MRI−CGCM3
NorESM1−M
Mean

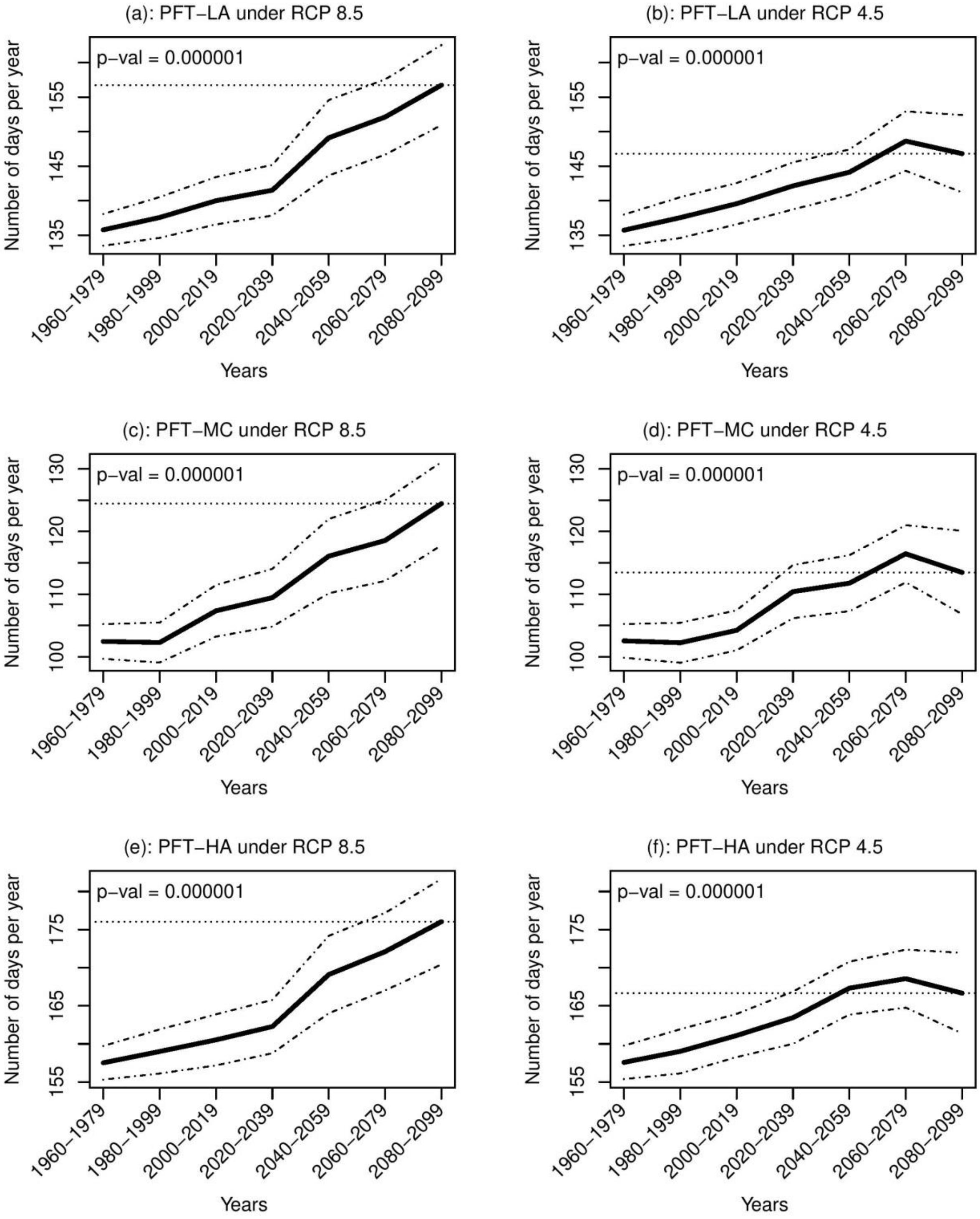

Fig.4 Temporal changes in average number of days per year of live fuel moisture content below 79% (black solid line) and 95% confidence interval (black dash-dot line) from ~~1950~~ 1960 to 2099 for three PFTs (refer to Figure 1 for explanation of the PFTs) under climate scenario RCP 4.5 and 8.5 with 20 Earth System Models considering all climatic variables changes. The P values were calculated using bootstrap sampling to test whether the number of days across

different models during the future period (~~2075~~2080–2099) was significantly higher than that during the historical period (~~1950~~1960-1999). The grey horizontal dotted line represents the ensemble mean for ~~2075~~2080–2099.

(a): PFT_LPAH below 79%

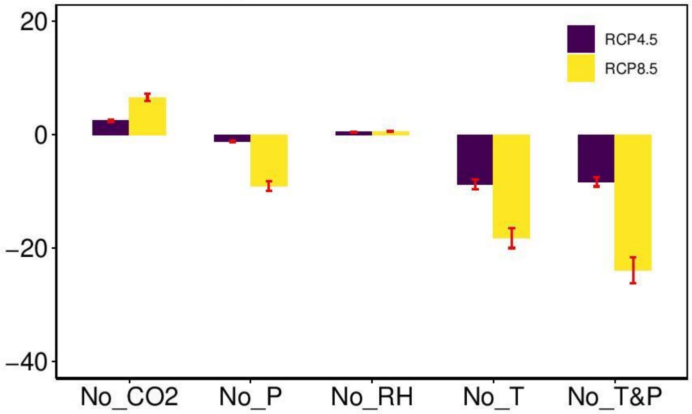

(b): PFT_MPCH below 79%

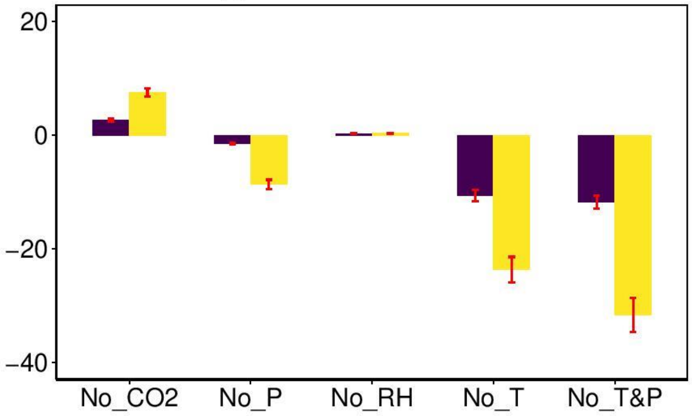

(c): PFT_HPAH below 79%

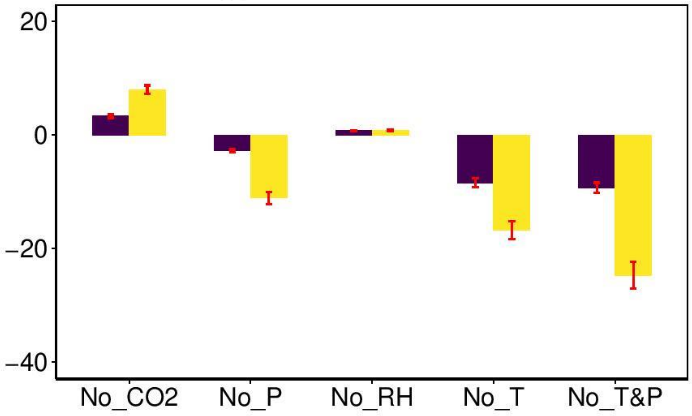

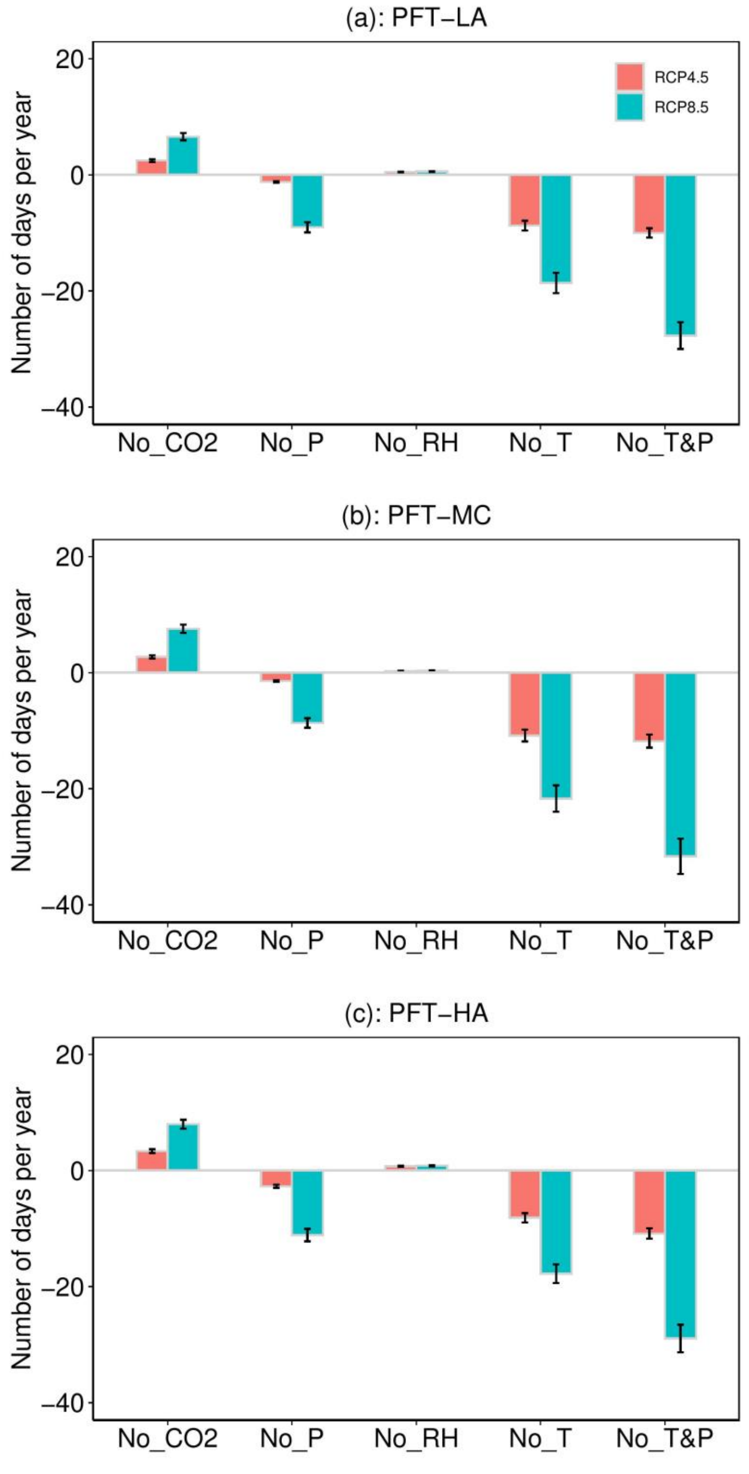

Fig.5 Differences on number of days per year of live fuel moisture content below 79% from ~~2075~~ 2080 to 2099 for three PFTs (refer to Figure 1 for explanation of the PFTs) under climate scenario RCP 4.5 and 8.5 between considering all climatic variables changes and without considering CO_2, precipitation, temperature, precipitation & temperature, relative humidity changes.